


Electrocatalysts based on MoS₂ and WS₂ for hydrogen evolution reaction: An overview

Tuan Van Nguyen¹ | Mahider Tekalgne¹ | Thang Phan Nguyen² |
 Quyet Van Le³ | Sang Hyun Ahn¹ | Soo Young Kim³ 

¹School of Chemical Engineering and Materials Science, Chung-Ang University, Seoul, Dongjak-gu, Republic of Korea

²Department of Chemical and Biological Engineering, Gachon University, Seongnam-si, Gyeonggi-do, Republic of Korea

³Department of Materials Science and Engineering, Institute of Green Manufacturing Technology, Korea University, Seoul, Seongbuk-gu, Republic of Korea

Correspondence

Sang Hyun Ahn, School of Chemical Engineering and Materials Science, Chung-Ang University, 84 Heukseok-ro, Seoul 06974, Dongjak-gu, Republic of Korea.
 Email: shahn@cau.ac.kr

Soo Young Kim, Department of Materials Science and Engineering, Institute of Green Manufacturing Technology, Korea University, 145 Anam-ro, Seoul 02841, Seongbuk-gu, Republic of Korea.
 Email: sooyoungkim@korea.ac.kr

Funding information

National Research Foundation of Korea, Grant/Award Numbers: 2017M3D1A1039379, 2021R1A4A3027878, 2022M3H4A1A010, 2020H1D3A1A04081409

Abstract

Recently, hydrogen energy has been significantly investigated by numerous technologies. To date, noble platinum group metals have often been employed to fabricate working electrodes for hydrogen evolution reaction (HER). Therefore, the demand of highly active HER catalysts based on effective and lower-cost materials is becoming more and more critical. Transition metal dichalcogenide (TMD) materials could be one of the most suitable materials for these requirements because they possess numerous unique mechanical, electronic, and chemical characteristics that are greatly beneficial for HER processes. Among many TMD materials, tungsten disulfide (WS₂) and molybdenum disulfide (MoS₂) are the most well-known TMD materials which have been intensively studied for different applications, including HER, batteries, and supercapacitors. In this review, we tried to cover the HER mechanism of catalysts and their parameters. Besides that, the structures, properties, preparation, and HER performance of catalyst materials based on WS₂ and MoS₂ are comprehensively discussed. After that, the challenges and future trends of catalysts based on WS₂ and MoS₂ for HER are also considered.

KEYWORDS

electrocatalyst, HER, MoS₂, TMD, WS₂

1 | INTRODUCTION

On the basis of the dimensions of materials, they can be categorized into 0D, 1D, 2D, and 3D materials.^{1–3} Zero-dimensional (0D) materials that are nanosized primarily consist of fullerenes, organic molecules, quantum dots,

and atomic clusters. One-dimensional (1D) materials with nanosized diameters include nanotubes, nanofibers, and nanowire structures. Two-dimensional (2D) nanomaterials exhibit a layer thickness of less than a few nanometers and can be layered together to create new materials with special structures. These materials show

This is an open access article under the terms of the Creative Commons Attribution License, which permits use, distribution and reproduction in any medium, provided the original work is properly cited.

© 2023 The Authors. *Battery Energy* published by Xijing University and John Wiley & Sons Australia, Ltd.

plate structures, such as graphene, transition metal dichalcogenides (TMDs), nanolayers, and nanofilms. Three-dimensional (3D) nanomaterials are materials that are not constrained to the nanoscale in any dimension. Three-dimensional materials could exhibit their morphologies in various shapes, including bulk powders, dispersions of nanoparticles, bundles of nanowires, nanotubes, and multi-nanolayers. Among different materials, 2D materials exhibit numerous outstanding properties that are suitable for many technologies.^{4–8} The first report concerning 2D materials was published on graphene in 2004, which are materials with thicknesses between 0.4 and 1.5 nm.^{9–11} Besides that, the weak interaction between basal planes of two layers (van der Waals forces—vdW forces) could lead to various unique physical or chemical properties. The vdW force is a distance-dependent interaction between atoms and molecules. The vdW forces can be repulsive or attractive forces which are highly dependent on the molecular surface area as well as the distance between molecules. The distances between layers ranging from 0.4 to 0.6 nm are ideal for the vdW forces to create ideal layered materials. The biggest advantage of 2D materials is that different thin layers can be integrated or stacked together to modify or prepare new heterostructures.¹² Therefore, 2D heterostructures with numerous structures can be prepared in which synergistic effects between different layers are formed. The synergistic effects of the heterostructure catalysts are crucial factors for their application because they can significantly enhance the catalytic activities of the synthesized materials.^{13,14} Because of the layered structure, 2D materials could exhibit many unique characteristics, including larger active surfaces, smooth heterostructure interfaces, ultrafast carrier transport, and highly gate-tunable bandgaps.^{15–18} Electronic carriers such as electrons or phonons in 2D materials can be transported more easily in the basal plane compared with the movement of carriers between different layers. Consequently, the movement of phonons and electrons in 2D catalyst materials is strongly dependent on the 2D plane properties and nanosized thickness between layers, which could cause significant changes in the electronic and optical properties of 2D materials. This explains why various types of 2D materials have been prepared with different characteristics, including insulators–hexagonal boron phosphorus, semiconductor–TMD, and semimetal–black phosphorus.¹⁹ Along with the development of advanced technologies, semiconductors based on TMD materials have been extensively investigated because TMD materials are low-cost, easy process, earth-abundant materials with many unique properties. In the last decades, TMD materials have been applied for many technologies, such as medical treatment, CO₂

reduction, energy storage, and catalytic materials and sensors.^{20–28}

TMD materials can be expressed by the general stoichiometry MX_2 , where M is a metal in transition group, including Mo, W, Ti, or Nb, and so forth, and X is an element in chalcogen group, such as S, Se, or Te.^{29–31} Figure 1 shows the typical structure of TMD materials from different perspectives. As can be seen from Figure 1A,B, TMD materials normally exist in two typical structures: 1T and 2H. In both 1T and 2H structures, TMD monolayers are formed with three layers of $X-M-X$ in which there is a hexagonally packed plane of metal atoms sandwiched between two planes of chalcogen atoms that are covalently bonded to the transition metal atoms. Transition metal atoms can have either octahedral or trigonal prismatic coordination. Because of the partially filled d-subshell in the outer shell of metal atoms, the different electronic behavior of TMD arises from the progressive filling of the nonbonding d-bands by transition metal electrons. Therefore, TMD materials could change their electronic properties from semiconducting to superconducting depending on their chemical compositions. In particular, group-VI TMD monolayers, such as MoS₂, WS₂, MoSe₂, and WSe₂, exhibit semiconductor behavior, with a direct bandgap in the range of 1–2 eV. In contrast, TMD multilayers or bulk TMD materials own an indirect bandgap.^{32–34} As shown in Figure 1C–F, the structure of TMDs is observed clearly on many sides of view. It is clear that the TMDs possess the similar crystal structure and different physical characteristics, such as bandgap, thermoelectric conversion, and light–matter interaction. However, by the stacked heterostructures as shown in Figure 1G, different layers of TMDs could form numerous materials which vary dramatically the characteristics of prepared materials, including photovoltaic properties, thermal transmission, elasticity, and catalysis. Due to the d-band of metal atoms, sandwiched structure, layered materials caused by vdW forces, TMD materials possess various advantages, such as nanometer thickness, direct bandgaps, strong spin–orbit coupling, and favorable electronic and mechanical properties. These properties are beneficial for many electrochemical fields, including oxygen evolution reaction, photoelectrochemistry, hydrogen evolution reactions (HERs), batteries, and supercapacitors.^{35–41} In Figure 1H,I, the layered structure of two typical TMD–tungsten disulfides (WS₂) and molybdenum disulfide (MoS₂) have been illustrated.

In recent decades, the energy crisis has become increasingly critical. Hydrogen energy is a great solution because it is an earth-abundant, eco-friendly, and renewable energy source. Numerous efforts have been made to produce hydrogen gas for various technologies on an industrial scale.^{47–52} Among the many great catalytic

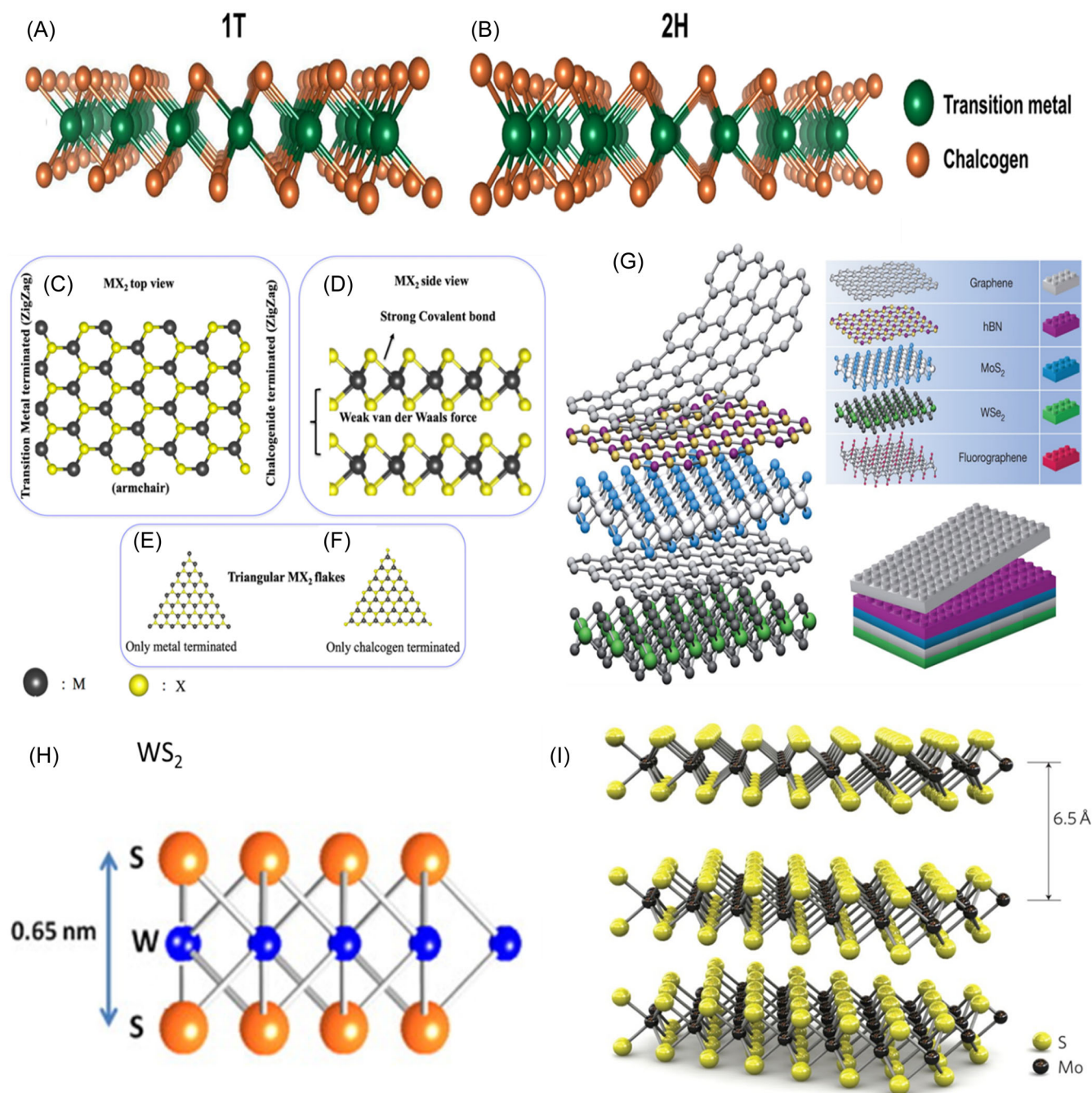


FIGURE 1 (A, B) 1T and 2H structures of transition metal dichalcogenide (TMD) materials. Reproduced with permission from Maghirang et al.,⁴² Copyright: 2019 Springer Nature. (C, D) top view and side view of MX₂, (E, F) transition metal and chalcogen terminated structures. Reproduced with permission from Ghatak et al.,⁴³ Copyright: 2020 Springer Nature. (G) differently layered TMD materials. Reproduced with permission from Geim and Grigorieva,⁴⁴ Copyright: 2013 Springer Nature. (H) structure of WS₂. Reproduced with permission from Suryawanshi et al.,⁴⁵ Copyright: 2015 Elsevier. And (I) structure of MoS₂. Reproduced with permission from Radisavljevic et al.⁴⁶ Copyright: 2011 Springer Nature.

materials, WS₂ and MoS₂ have been considered as the two flagship catalysts for the HER process with superior catalytic activities.^{53–55} To fully understand the HER mechanism, numerous efforts from scientists, as well as the development of advanced technologies to precisely control the process are required. Most scientists agree that the HER performance of catalysts significantly depends on

the electroconductivity and the active sites of the materials. For TMD materials, the active sites are usually considered as the edges of the catalysts. Therefore, the more edges catalysts possess, the higher HER performance could be exhibited. Due to their layered structure, which presents numerous active sites, TMD materials have been extensively studied for the HER process. The mechanisms

of the HER processes based on MoS₂ and WS₂ catalysts could be depicted in Figure 2A,B which are in good agreement with previous reports.^{56,57} As can be seen, the mechanisms of MoS₂ and WS₂ are highly similar. The H⁺ ions in the solution are reduced by electrons from the cathode electrode, which is made from the synthesized catalysts. For that reason, electrode catalysts with more active sites, high conductivity, and large surface areas are ideal materials for preparing cathode electrodes where hydrogen gases can be released. In fact, as with many TMD materials, the electronic conductivity of MoS₂ and WS₂ is still poor that is the huge challenge to apply MoS₂ and WS₂ as practical catalysts for large scale. In the last decades, considerable efforts and various strategies have been intensively applied to improve the HER performance of electrode catalysts based on both MoS₂ and WS₂.

In this work, we focus on the fundamental mechanism of HER process with theoretical calculations related to the HER process. First, different advanced techniques have been applied to explore the catalytic mechanisms and the electrochemical HER from the viewpoint of computational quantum chemistry. Second, the structures and characteristics of MoS₂ and WS₂ catalysts are comprehensively summarized. In the subsequent sections, we mainly discuss the state-of-the-art advances in HER using

electrocatalysts electrodes based on MoS₂ and WS₂ materials. Synthesis protocols and new approaches to prepare MoS₂ and WS₂ materials were encapsulated. Different techniques to improve the efficiency of catalysts have been summed up including the increase of intrinsic activity and the increase of active sites of catalysts based on MoS₂ and WS₂ materials. The relationship between the catalytic activity, morphology, structure, composition, and synthetic method was also deeply reviewed. Finally, the challenges, perspectives, and research trends in future HER-related catalysts for the development of sustainable and clean hydrogen energy are put on the table. On the basis of the valuable analysis and the significant developments of technologies, catalyst materials based on MoS₂ and WS₂ could be considered as great candidates which can make a breakthrough in HER catalyst development.

2 | HER MECHANISM OF CATALYSTS

To date, electrochemical water splitting or hydrolysis of water has been considered one of the most promising approaches to produce hydrogen gas, which can be employed to store renewable electricity in the form of

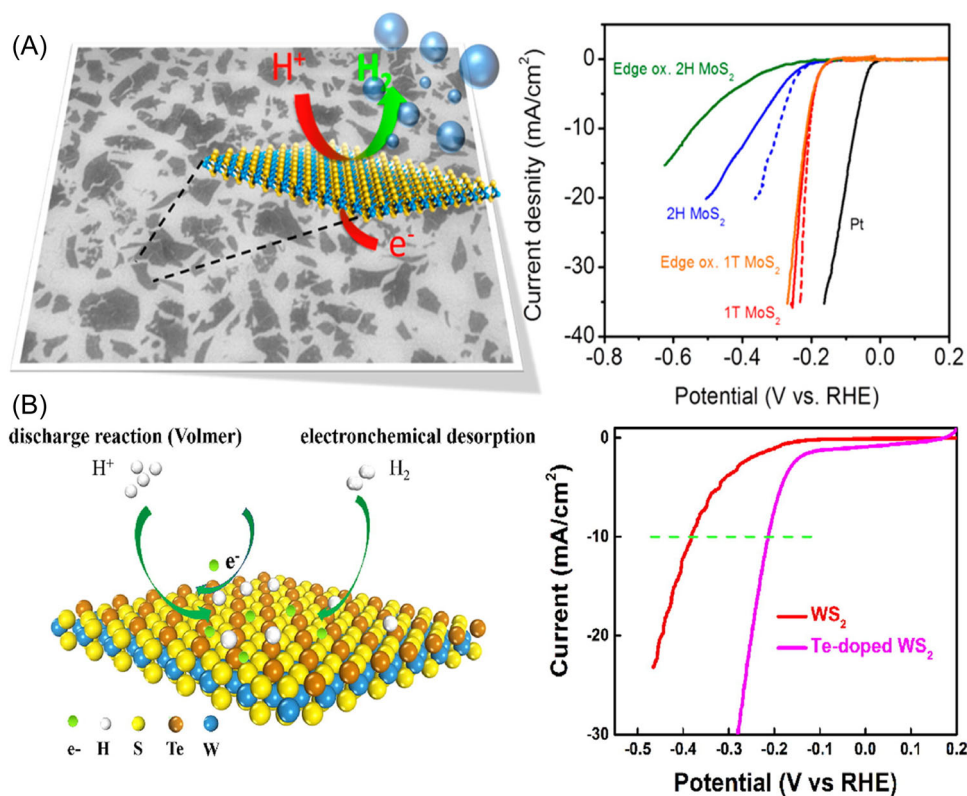
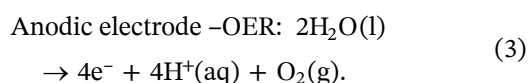
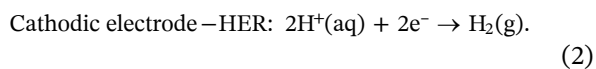
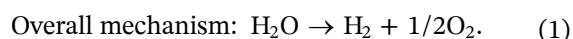


FIGURE 2 Mechanism of hydrogen evolution reaction process based on (A) MoS₂. Reproduced with permission from Voiry et al.,⁵⁸ Copyright: 2013 American Chemical Society. And (B) WS₂. Reproduced with permission from Pan et al.⁵⁹ Copyright: 2020 Elsevier. RHE, reference hydrogen electrode.

hydrogen energy or apply for hydrogen energy technologies. Figure 3 shows the overall water-splitting mechanism using a potential. Under the applied potential, water molecules are hydrolyzed to free H₂ at the cathodic electrode and O₂ at the anodic electrode. However, it is challenging to produce H₂ and O₂ on a commercial scale because of the high overpotential. This overpotential is the excess energy required to overcome the self-ionization of water and sluggish reaction kinetics of the HER. To overcome the self-ionization of pure water, the HER process is carried out in an electrolyte that uses acidic or alkaline media. The kinetic energy barrier was decreased by using electrode catalysts. The HER activity in acidic media was significantly improved compared with that in alkaline media.⁶⁰ Typically, noble and scarce catalysts, including platinum-based catalysts, have been employed to prepare cathodic electrodes for H₂ production. Therefore, the synthesis of electrode electrocatalysts that can be used in acidic media with low cost, high catalytic activity, and good durability for electrolytic water splitting is challenging. In the electrochemical water-splitting process, the overall mechanism as well as the reduction and oxidation at the cathodic and anodic electrodes can be described by the following equations^{61,62}:



Water splitting requires an energy input of $\Delta G = 237.13 \text{ kJ mol}^{-1}$ at standard pressure ($P = 100 \text{ kPa}$) and temperature ($T = 298 \text{ K}$) conditions.⁶⁴⁻⁶⁶ The theoretical input energy of this reaction corresponds to a thermodynamic voltage requirement of 1.23 V. In fact, because of the kinetic barrier for the process, splitting water needs higher power than the theoretical input to overcome the kinetic barrier, which is usually higher than 1.8 V.⁶⁷ The excess potential is overpotential η , which is needed to compensate for intrinsic activation barriers present on the surface cathode. To overcome the challenge, many solutions have been investigated. Among them, using electrocatalysts is a prominent pathway in which electrocatalysts play a vital role in increasing reaction rates and control processes in HER. Effective catalysts can reduce the energy barriers at each step of the process. To date, various electrocatalysts that can accelerate the reaction on electrode surfaces have been investigated. Therefore, the overpotential is an important factor for evaluating the activity of electrocatalysts. To save energy consumption, a superior catalyst requires a smaller excess potential for the HER to occur.⁶⁸⁻⁷⁰ In fact, the overpotential values of catalysts which are needed to generate a current density of 10 or 50 mA cm⁻² are often used to compare the catalytic activities of different catalysts.⁷¹

As previously mentioned, the HER is an electrochemical phenomenon which took place at cathodic reaction in electrochemical water splitting. The HER process involves intermediate hydrogen adsorption and desorption H₂ from the electrode surface, and the adsorption energy depends on the nature of the electrode materials used, as well as the kinetics of the HER. In the

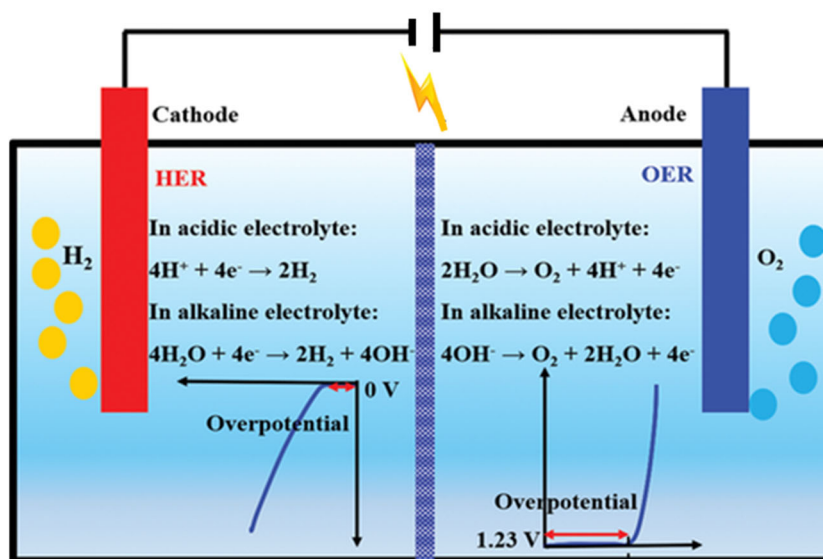
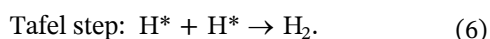
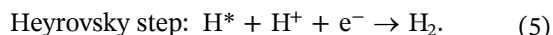
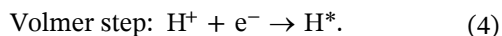
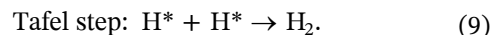
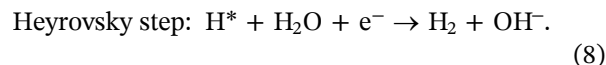
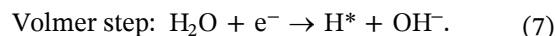


FIGURE 3 Water-splitting process. Reproduced with permission from Zhang et al.⁶³ Copyright: 2019 John Wiley and Sons. HER, hydrogen evolution reaction; OER, oxygen evolution reaction.

HER process, two intermediate hydrogens in electrolyte are reduced by two electrons from cathode surface under applied potential to release H_2 . There are several mechanisms which have been suggested to elucidate HER reaction mechanism. Among them, the most popular theory agrees that the reaction mechanism of the HER process in acidic and alkaline solutions is related with the adsorption and/or desorption of intermediate hydrogen (H^*) which could be described by the Volmer–Heyrovsky or the Volmer–Tafel mechanism as follows^{72–74}:



In alkaline media, the reaction formula for the HER is represented as follows:



The different mechanisms of HER processes are illustrated in Figure 4. In which, step by step of HER processes takes place under acidic and alkaline conditions are shown. It is clear that the required energy for each process is not the same because of the different energy barriers of each step. Therefore, the optimized catalysts have been intensively investigated to accurately

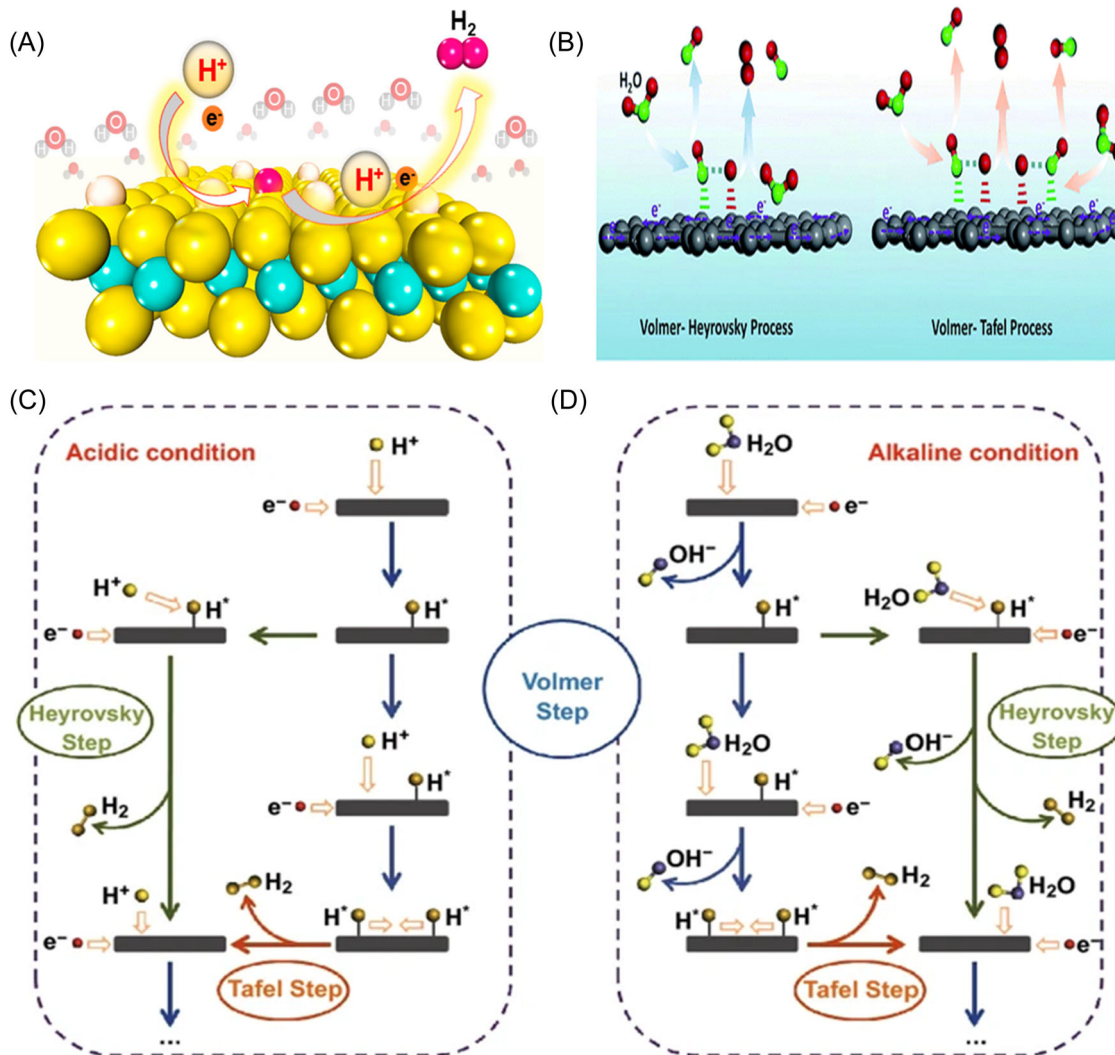


FIGURE 4 (A) The hydrogen evolution reaction (HER) mechanism in acidic media. Reproduced with permission from Tang et al.,⁷⁹ Copyright: 2016 American Chemical Society. (B) the HER mechanism in alkaline media. Reproduced with permission from Chen et al.,⁸⁰ Copyright: 2019 Royal Society of Chemistry. And schematic pathways for the HER under (C) acidic and (D) alkaline conditions. Reproduced with permission from Wei et al.⁸¹ Copyright: 2018 Springer Nature.

control the process. In fact, catalytic materials exhibit poor activity and lower efficiency in alkaline solutions much more than in acidic solutions. However, under acidic media, the used catalysts are less stable. For instance, the results indicate that the obtained reaction rate for the HER with Pt in an acidic environment is significantly higher than that under alkaline conditions. This is likely caused by the initial water dissociation process on the Pt surface is inefficient, which is shown in the Volmer step of the alkaline HER. This caused the poor HER performance of catalysts in alkaline media. Because of the high cost and poor stability of catalysts based on platinum metal groups, recently, numerous earth-abundant catalysts with good catalytic activities have been intensively studied. Among them, WS₂ and MoS₂ are excellent catalysts with high performance and superior stability in acidic environments.^{75–78} Therefore, the structures and characteristics of WS₂ and MoS₂, as well as the HER performance of electrocatalysts based on WS₂ and MoS₂, are mainly discussed in this review.

3 | PARAMETERS OF ELECTROCATALYTIC HER

3.1 | Overpotential

In the HER process, overpotential of catalysts is evaluated as one of the most crucial parameters for considering its catalytic performance. In addition to the current density and Tafel slope, the overpotential of each catalyst has been carefully investigated to determine the catalytic activity of the prepared materials. As mentioned above, for the HER process, an extra potential is required compared with the thermodynamic potential (E_{HER}). This value is considered to be the overpotential of the catalysts, as illustrated in

Figure 5A. Therefore, the applied potential for the HER process can be calculated as follows:

$$E = E_{\text{HER}} + iR + \eta, \quad (10)$$

where E_{HER} is determined by thermodynamics, iR is the Ohmic potential drop caused by the current flow in ionic electrolytes, and η is the overpotential of the catalysts.

Electrocatalysts are typically used to decrease the reaction overpotential for saving the supplied energy by activating intermediate chemical transformations. Therefore, a good catalytic material requires the lowest overpotential to achieve the highest efficiency of the process. In fact, η_{10} or η_{50} , which indicates the overpotential at a current density of 10 or 50 mA cm⁻² of catalysts, is usually calculated to compare the HER performance of materials (Figure 5B). A smaller η value suggests that the catalyst is more conductive and has higher HER activity. To calculate and compare the actual catalytic activity of the prepared materials, the synthesized catalysts must be loaded with a standard amount of catalyst on an electrode with a standard area electrode to evaluate the HER behavior in a standard process.

3.2 | Volcano plots

For the HER process in acidic media, the free-energy change between the cation (H⁺) and the formed material (H₂ gas) was calculated thermodynamically. This energy value is constant for all catalysts, since it is an intrinsic property of H₂. As mentioned above, the thermodynamically ideal catalyst exhibits the lowest overpotential for higher current densities. In electrocatalytic reactions, the chemical bonds of elements have been

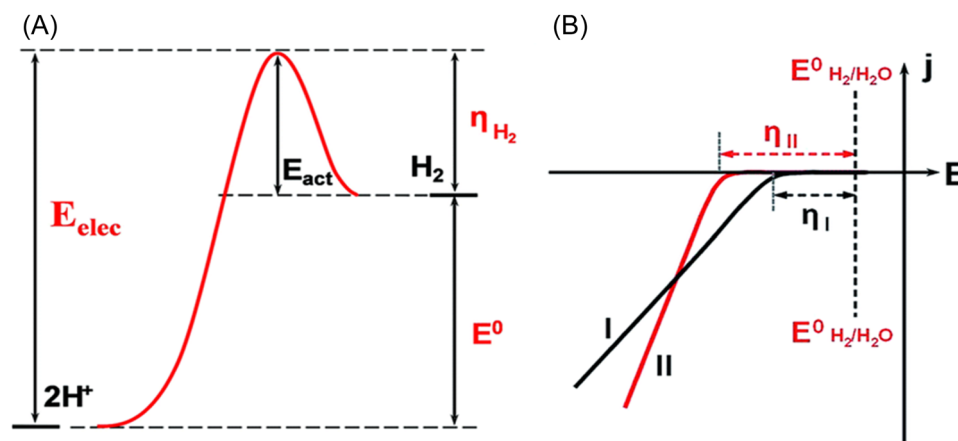


FIGURE 5 (A) Overpotential of the catalysts η and (B) comparison of onset overpotentials of two different electrocatalysts. Reproduced with permission from Zeng and Li.⁸² Copyright: 2015 Royal Society of Chemistry.

reconstructed to prepare new materials. Because of that, the HER process can be considered as bonded electron-transfer process. As per the statement in Sabatier's theory, which concludes that the binding energy between the catalysts and the reactants should be reasonable that means it is not too strong nor too weak. If the binding energy is too weak, the cation H^+ could be more difficult to attach to the cathode surface which causes the rate of reduced reaction to take place very slowly. In contrast, if the binding energy is too strong, the released H_2 product could be difficult to detach from the cathode surface. This could also form a bubble layer on the cathode surface which can stop the process. Therefore, the ideal catalyst is the one with zero binding energy between the catalyst and the intermediate H^* . In the HER process, the two steps of H^+ reduction and adsorbed H^* desorption on the cathode surface. The key HER parameter is hydrogen binding energy (HBE). As shown in Figure 6A, a catalyst surface with very weak hydrogen binding (H-binding) cannot efficiently initiate the reaction. On the other hand, a catalyst surface with very strong binding would prohibit the desorption of H^* to generate H_2 . For an ideal HER electrocatalyst, H-binding should be moderate to balance the two elementary steps. To calculate the HBE, recently, density functional theory (DFT) has been intensively studied to calculate the hydrogen-binding-free energy of a catalyst (ΔG_{H^*}). The ΔG_{H^*} of MoS_2 and WS_2 and many other catalysts are shown in Figure 6B. It is clear that the Volcano peak is located at $\Delta G_{H^*} = 0$, which is the ideal ΔG_{H^*} value of the catalyst. In which, Pt has a ΔG_{H^*} value closest to the peak position of the Volcano curve. This indicates that Pt-based catalysts are the most effective for electrochemical applications. Nevertheless, catalysts based on Pt metal groups have significant drawbacks, including high cost and low stability. Therefore, numerous efforts

have been devoted to prepare catalysts with zero ΔG_{H^*} , low cost, easy process, and stability.

3.3 | Tafel slope

Along with overpotential, the Tafel slope is another critical factor for evaluating the HER performance of catalysts. Microkinetic analysis and the rate-determining step (RDS) of the HER process could be explained by using the Tafel value. The Tafel slope value is often studied to compare the electrocatalytic activities of catalysts and explain the mechanism of the HER performance. A smaller Tafel slope means that a lower overpotential is required to deliver the same current density increment, which means that the electron-transfer kinetics of the reduction-oxidation process are faster. A high-performance electrocatalyst exhibits a high-exchange current density and a small Tafel slope. To the best of our knowledge, Pt is the most effective catalyst, which shows the smallest Tafel slope of approximately 33 mV dec^{-1} . The Tafel slope values of other synthesized catalysts have been usually compared with that of Pt. The Tafel slope is used to represent the correlation between the catalytic current density (j) and overpotential η , which can be inferred from the Butler-Volmer kinetic model using the following equation⁸⁵⁻⁸⁷:

$$j = j_0 [-e^{-anF\eta/RT} + e^{(1-\alpha)nF\eta/RT}], \quad (11)$$

where η is the overpotential of the reaction process, j is the current density, j_0 is the exchange current density, α is the charge-transfer coefficient, n is the number exchanged electrons of process, F is the Faraday constant, R is the ideal gas constant, and T is the reaction temperature.

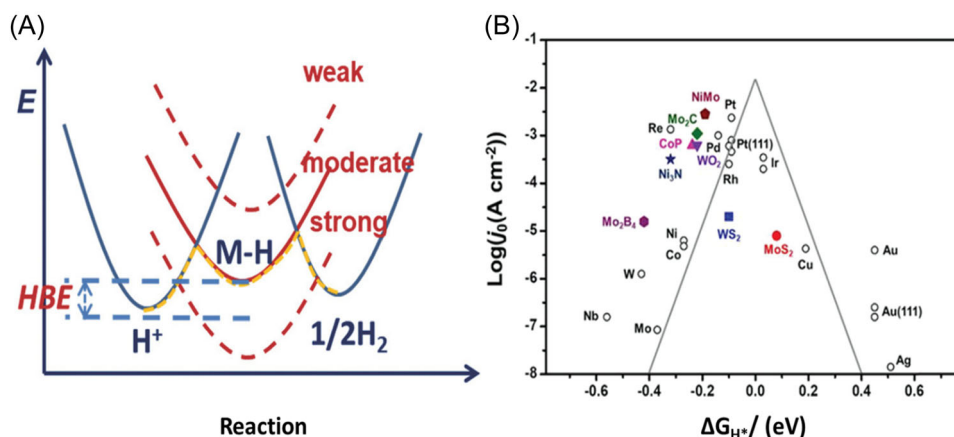


FIGURE 6 (A) The mechanism of electrocatalytic HER. Reproduced with permission from Gao et al.,⁸³ Copyright: 2018 John Wiley and Sons. (B) Volcano plot of MoS_2 and WS_2 and their corresponding ΔG_{H^*} . Reproduced with permission from Yu et al.⁸⁴ Copyright: 2019 Elsevier. HBE, hydrogen binding energy; HER, hydrogen evolution reaction.

If overpotential is small ($\eta < 0.005$ V), the Butler–Volmer equation could be calculated as

$$\eta = \left(\frac{RT}{\alpha n F j_0} \right) j. \quad (12)$$

At a higher overpotential ($\eta > 0.05$ V), the Butler–Volmer equation can be expressed as

$$\eta = a + b \log(j) = \frac{-2.3RT}{\alpha n F} \log j_0 + \frac{2.3RT}{\alpha n F} \log j. \quad (13)$$

The linear relationship between the overpotential η and $\log j$ is calculated as Tafel slope value:

$$\text{Tafel slope value: } b = \frac{2.3RT}{\alpha n F}. \quad (14)$$

The Tafel slope can be obtained from the linear part of the Tafel plot by plotting the overpotential using Equation (14). On the basis of the obtained Tafel slope, the mechanism of the HER process could be analyzed. Figure 7 shows different RDSs of the HER process. The RDS of the process could be Volmer reaction, Heyrovsky reaction, and Tafel reaction which is corresponded with a Tafel slope of ~ 120 , ~ 40 , and ~ 30 mV dec $^{-1}$, respectively. On the basis of the Tafel slope, the mechanism of the HER process could be elucidated.

3.4 | Electrochemical impedance spectroscopy (EIS)

The conductivity of catalysts applied for the HER is also a critical parameter for evaluating the activity of materials.

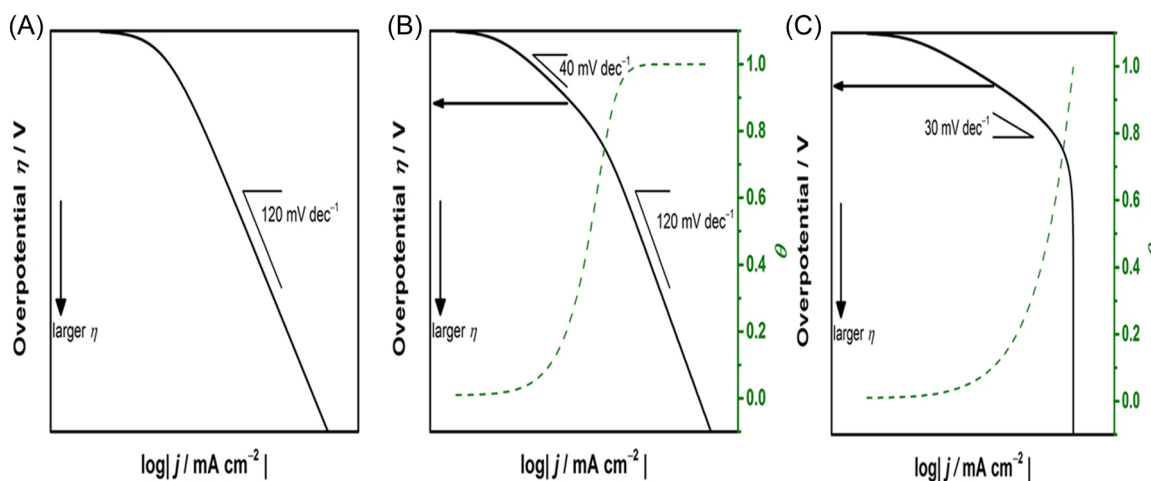


FIGURE 7 Tafel slope for hydrogen evolution reaction as a rate-determining step. Reproduced with permission from Shinagawa et al.⁸⁷ Copyright: 2015 Springer Nature.

As mentioned above, the HER involves the adsorption process of H* onto the electrode surface and the desorption process of H₂ from the electrode surface. The Langmuir adsorption model is often used to explain the mechanism of the adsorption process of H* onto the electrode surface. Recently, EIS has been intensively applied to study the changes in capacitance and interfacial electron-transfer resistance at the electrode surface. Therefore, EIS techniques could be employed to evaluate the rates and kinetics of adsorption and desorption processes of H₂ from electrode surfaces. The EIS profiles of hybrid materials between graphene oxide (GO) with CH₃NH₃PbI₃ (PSK) are described in the

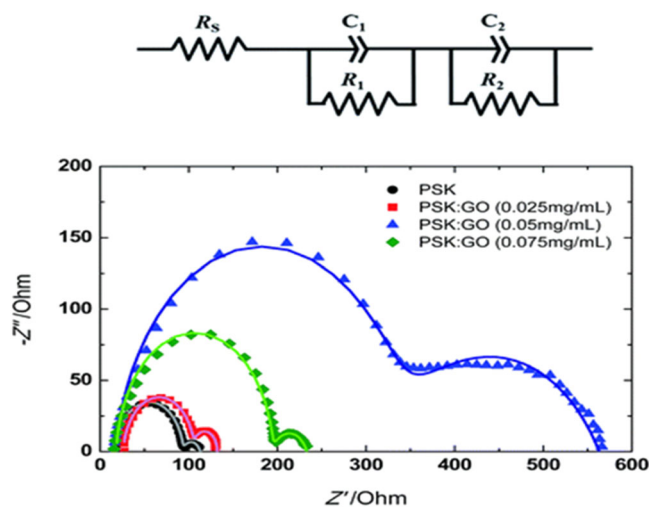


FIGURE 8 Nyquist plots obtained from the EIS of the pristine PSK and PSK:GO hybrid composite. Reproduced with permission from Chung et al.⁸⁸ Copyright: 2017 Royal Society of Chemistry. EIS, electrochemical impedance spectroscopy; GO, graphene oxide; PSK, CH₃NH₃PbI₃.

Nyquist Plot in Figure 8. In which, the internal electrical processes of materials were discussed. It can be seen that the equivalent circuit is composed of constant-phase elements and charge-transfer resistances. The charge-transfer resistances include the wire connection resistance (R_s), the resistance between the active material and electrolyte (R_1), and resistance between the active material and glassy carbon electrode (R_2). For the HER, a smaller R_1 value suggests a faster reaction rate, leading to a smaller overpotential.

3.5 | Stability of catalysts

The prolonged working time of the catalyst materials is also a vital factor in catalyst studies. The more stable the catalysts, the lower the cost of hydrogen energy; and the stability of the material is considered to be a key factor in evaluating catalytic activity. Meanwhile, the cyclic voltammetry (CV) test revealed the stability of the catalytic material after repeated cycling. The chronoamperometry (CA) and chronopotentiometry (CP) tests show the dependence of the catalyst stability on testing time at a potential or constant current density, respectively. Normally, CV tests are conducted for at least 1000 cycles to observe the changes in the linear sweep voltammetry (LSV) curves. Smaller changes in LSV curves indicate better stability of the catalyst. In the CA tests, the current density changes under fixed potential with time were carefully studied. In contrast, in the CP tests, the changes of overpotential at a constant current density could be intensively investigated. Both the CA or CP tests for catalysts are usually surveyed

from 10 to 60 h. There are smaller changes in the CA and CP curves which indicate better stability of catalysts. Figure 9A,B shows the stability of catalysts for HER application by CV and CP tests, respectively. The stability of the catalysts is investigated by CV tests for 1000 cycles and CP measurements for 10 h.

3.6 | Turnover frequency (TOF)

To evaluate the HER performance, the TOF, which relates to the generation of products, is also a key parameter to consider. TOF can be considered as an accurate criterion of the intrinsic activity of catalysts, which can be employed to evaluate how efficient a catalyst is for HER performance. In 1968, Michel Boudart first reported a novel method to evaluate the catalytic rate of a catalyst in terms of the TOF. In which, the TOF value is calculated by the amount of product formed or the reactant consumed per unit time by a standard area. To date, the TOF concept has been quite complicated, and it still requires common agreement from researchers.⁹⁰ Recently, the TOF value was commonly agreed by many researchers as the total number of molecules transformed into the desired product per catalytic site per unit time. There are several methods to calculate the TOF using the following equations⁹¹:

$$\text{TOF} = \frac{j \times N_A}{F \times n \times I}, \quad (15)$$

$$\text{TOF} = \frac{i \times N_A}{A \times F \times n \times I}, \quad (16)$$

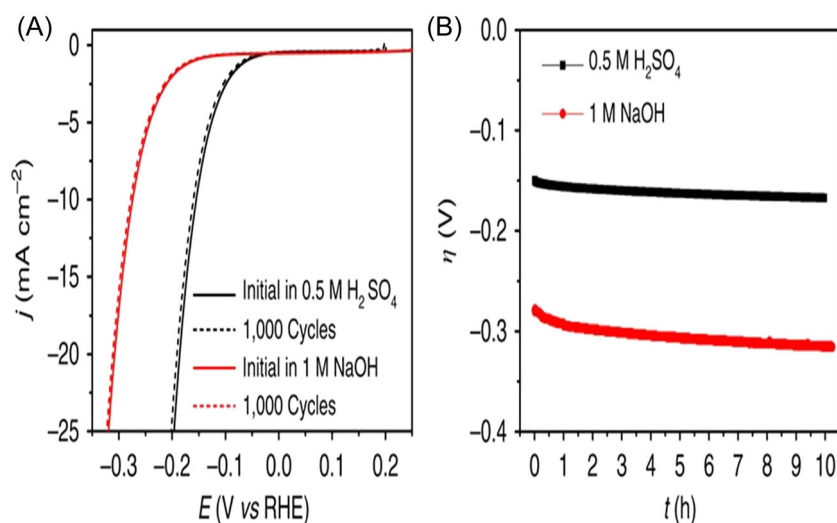


FIGURE 9 Stability tests of cobalt-nitrogen-doped graphene under acidic and alkaline media. (A) LSV curves after 1000 CV cycles and (B) plot of η - t curves for cobalt-nitrogen-doped graphene under acidic and alkaline media at constant current density 10 mA cm^{-2} . Reproduced with permission from Fei et al.⁸⁹ Copyright: 2015 Springer Nature. CV, cyclic voltammetry; LSV, linear sweep voltammetry; RHE, reference hydrogen electrode.

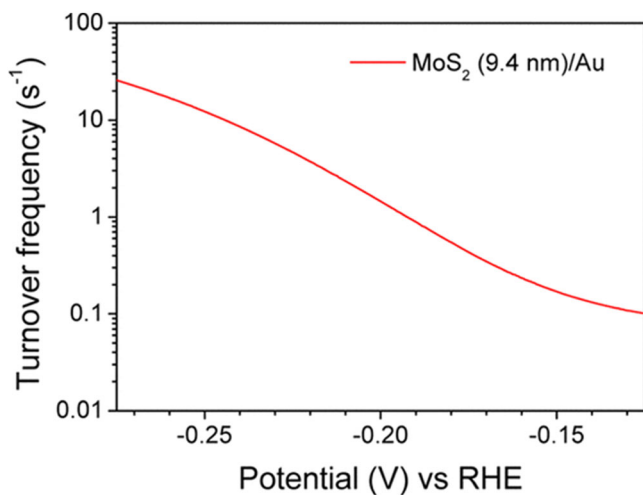


FIGURE 10 Turnover frequency of amorphous MoS₂ catalysts. Reproduced with permission from Shin et al.⁹² Copyright: 2015 American Chemical Society. RHE, reference hydrogen electrode.

$$\text{TOF} = \frac{j}{F \times n \times x} \quad (17)$$

In Equation (15), j , N_A , F , n , and I represent the current density, Avogadro constant, Faraday constant, number of electrons transferred to generate one molecule of the product, and surface concentration or exact number of active sites catalyzing the reaction (m^{-2}), respectively. i and A in Equation (16) represent the current and area of the electrode, respectively, and x in Equation (17) stands for the number of moles of active sites available for the catalysis. As for the HER process, $n = 2$, which is the number of electrons transferred when a molecule of H₂ gas is formed. Figure 10 shows the calculated TOF of the amorphous MoS₂ thin film (thickness 9.4 nm) deposited on Au film using the atomic layer deposition (ALD) technique.

In fact, it is difficult to precisely calculate the TOF of the catalyst, especially for some hybrids or heterostructure materials. The different properties of each catalyst and the complicated mechanism of electrocatalytic process are the main challenges to calculate exactly TOF value. Although the calculated TOF is relatively imprecise, however, it is still considered as a helpful parameter to compare the catalytic activities of materials.

3.7 | Surface area and pore structure

In the HER process, hydrogen gas is released from the surface of the cathode. Therefore, the larger the cathode surface area, the more hydrogen gas escapes during hydrolysis. Therefore, catalytic materials with rough

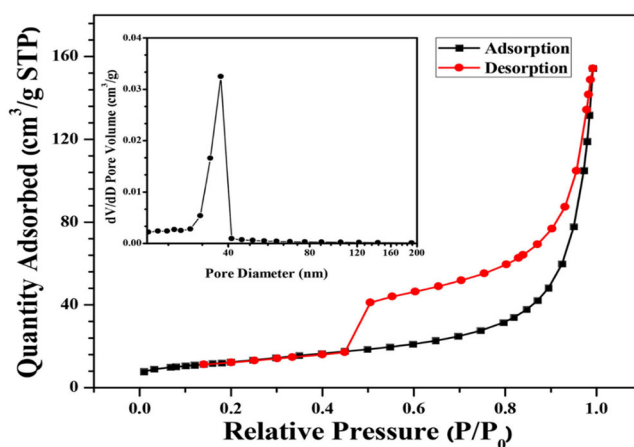


FIGURE 11 N₂ adsorption–desorption isotherm of the MoS₂–rGO and pore size distribution of the MoS₂–rGO nanocomposite. Reproduced with permission from Xie and Xiong.⁹³ Copyright: 2017 Elsevier. rGO, reduced graphene oxide.

and perforated morphologies are more suitable for water splitting. Moreover, the larger the pore size, the easier it is for the hydrogen gas to be liberated. To determine the surface area and pore size of the catalysts, the Brunauer–Emmett–Teller surface area using the nitrogen adsorption–desorption isotherms and Barrett–Joyner–Halenda for the pore size distribution of the materials are measured and calculated, as done in a previous study, and shown in Figure 11. The high specific area and large total volume provided more surface-active sites and pore channels, resulting in good adsorption performance.

3.8 | Electronic density of state (DOS)

Electronic DOS is a crucial parameter in modern electronic structure theories. In theory, DOS controls the distribution of energy levels that can be occupied by electrons in a quasiparticle picture. In solid state physics and condensed matter physics, DOS of a system describes the number of modes per unit frequency range. By the obtained DOS value, the electrical and optical properties of the materials could be elucidated by the bandgap and effective masses of carriers. In recent decades, WC and W₂C have been considered a great catalytic material that can be substituted for the Pt group.⁹⁴ The catalytic activity of WC and W₂C is considerable because of its modified d-band electron structure with a greater DOS near the Fermi level upon the incorporation of carbon interstitial atoms. To compare the catalytic properties of WC and W₂C, the DOS was calculated. Figure 12 compares the DOS of the W and C atoms in prepared WC and W₂C materials. As

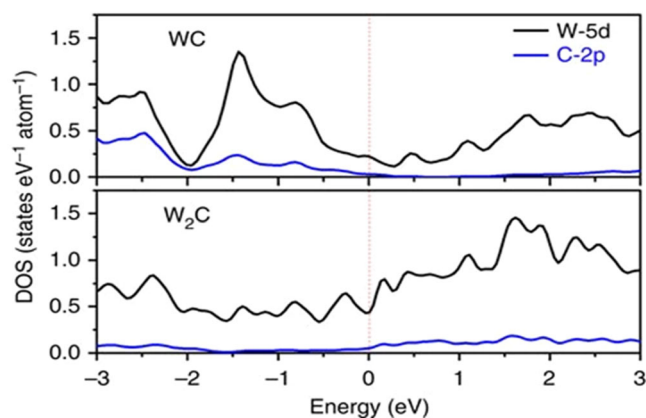


FIGURE 12 Calculated density of state (DOS) of W and C atoms in W_2C and WC. Reproduced with permission from Gong et al.⁹⁵ Copyright: 2016 Springer Nature.

can be seen, the calculated DOS data confirmed the considerable W 5d contribution at the Fermi level. The electronic DOS of W_2C near the Fermi level is larger than that of WC. This result can be interpreted by the higher W concentration in W_2C , which could enhance the metallicity. Therefore, the carrier density of W_2C is significantly improved compared with that of WC. This improvement could benefit the HER process because of the increase in charge transfer. It is also confirmed by d-band theory, it states that a lower d-band center results in weaker bonding between the catalyst and adsorbate. The obtained DOS indicates that the catalytic activity of W_2C far exceeds that of WC.

4 | WS_2 AND MoS_2 : STRUCTURE AND PROPERTIES

4.1 | Crystallinity and chemical bonding of WS_2 and MoS_2

The crystallinity and structure of WS_2 and MoS_2 are highly similar, as confirmed by X-ray powder diffraction (XRD) and Raman spectroscopy in Figure 13. The chemical bonding and chemical components of WS_2 and MoS_2 are also shown in Figure 13. The corresponding binding energy levels of atoms on the surface of the W–S and Mo–S bonds are presented in Figure 13A–D. As can be seen, in pure MoS_2 , the outer layer of the Mo atom is Mo 3d, which has two main energy levels, Mo $3d_{5/2}$ and Mo $3d_{3/2}$, which have binding energies of 231.9 and 229.8 eV, respectively. Similarly, in the pure WS_2 catalyst, the outer layer of the W atom is W 4f, which has two main energy levels, W $4f_{7/2}$ and W $4f_{5/2}$, which have corresponding binding energies of 34.2 and

32.1 eV. The crystallinity and the chemical bonding of WS_2 and MoS_2 have been confirmed by the XRD patterns and Raman spectra, as shown in Figure 13E,F. The synthesized WS_2 shows various peaks that can be indexed to the standard JCPDS card-08-0237. The synthesized MoS_2 also shows similar peaks located in a similar position, and is assigned to the JCPDS card-37-1492. A significant difference between WS_2 and MoS_2 is regarding the Raman peaks, presented in Figure 13F. The E_{2g}^1 mode is an in-plane optical mode, whereas the A_{1g} mode corresponds to the out-of-plane vibrations of sulfur atoms. The Raman peaks of WS_2 are centered at approximately 350 and 421 cm^{-1} , which are attributed to the optical phonon modes E_{2g}^1 and A_{1g} . In contrast, E_{2g}^1 and A_{1g} of MoS_2 are centered at 375 and 403 cm^{-1} , respectively.

4.2 | Structural characteristics of WS_2 and MoS_2

In addition to similar crystallinities, the structures of WS_2 and MoS_2 are also similar. The detailed structures of WS_2 and MoS_2 are presented in Figure 14A, and the calculated structural parameters, binding energies, and energy bandgaps of the WS_2 and MoS_2 catalysts are listed in Table 1, which were calculated and reported in previous studies.^{99–101}

Figure 14B shows different phases from 1T and 2H to 3R for MoS_2 and WS_2 , where the number counts the layer material per unit cell. Besides that, the character denotes for the type of symmetry, including T is tetragonal (D_{3d} group), H indicates hexagonal (D_{3h} group), and R stands for rhombohedral (C_{3v}^5 group). Among them, the 1T phase owns the metallic properties. In contrast, both the 2H and 3R phases present semiconducting characteristics. Compared with the 2H-phase, the 1T phase of catalysts based on MoS_2 and WS_2 exhibits the metallic properties with extraordinary electronic conductivity and larger interlayer spacing as well as more active sites along the basal plane. That means the catalytic activities of the 1T phase are more advanced compared with that of the 2H phase. In nature, MoS_2 and WS_2 are usually found in the 2H phase and the 2H phase also exhibits better stability compare with the 1T phase. A monolayer of MoS_2 or WS_2 possesses a lamellar S–Mo–S or S–W–S structure with a layer thickness of 0.65 nm. The monolayer of MoS_2 or WS_2 is formed by one layer of Mo or W atoms sandwiched by two layers of S atoms by covalent interactions. The different layers of MoS_2 and WS_2 could be held by weak vdW forces. If the structure of MoS_2 or WS_2 is trigonal prismatic, which will form a 2H

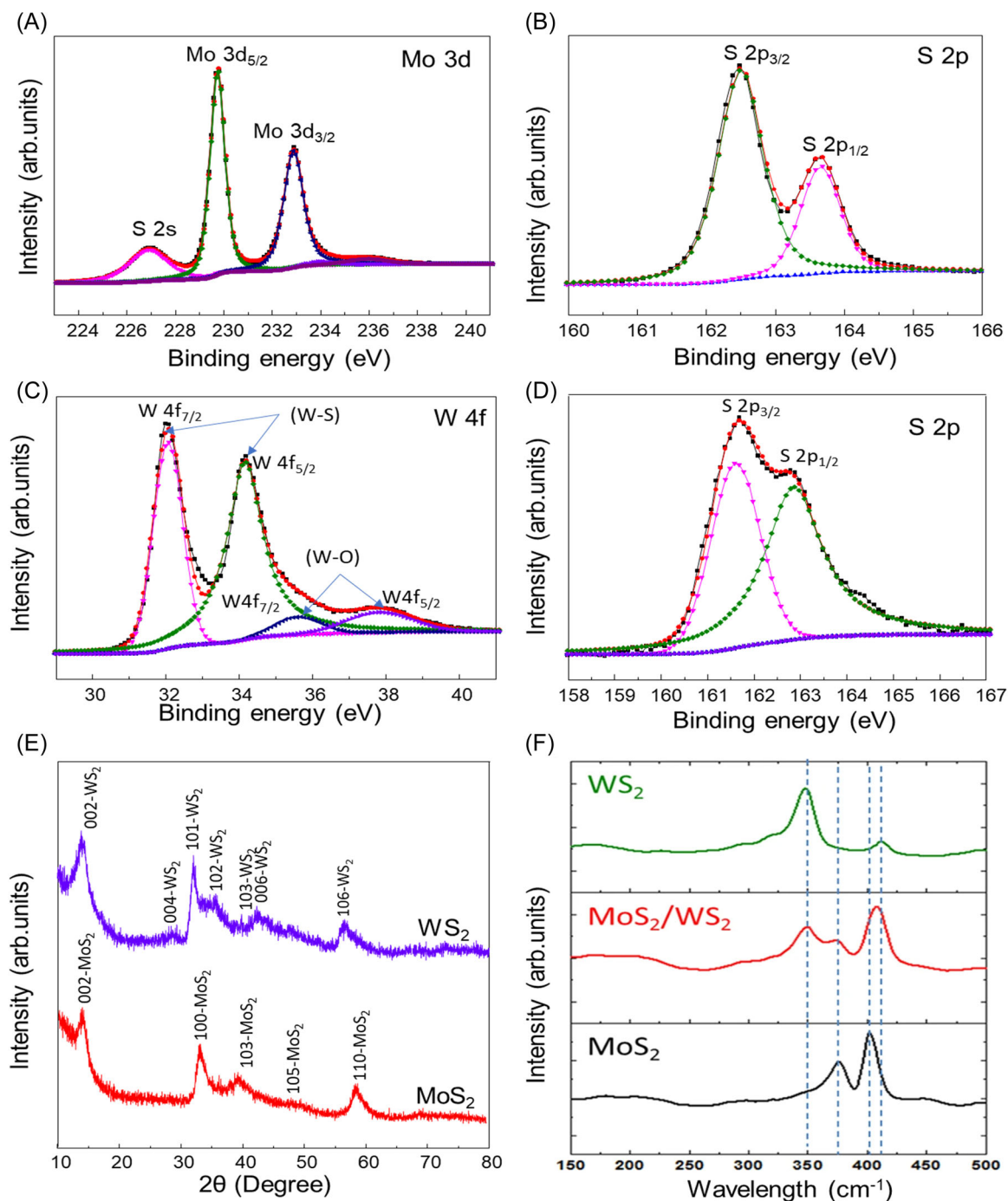


FIGURE 13 (A, B) Fitted high-resolution peaks of MoS₂ and (E) XRD patterns of MoS₂. Reproduced with permission from Van et al.⁹⁶ Copyright: 2022 John Wiley and Sons. (C, D) Fitted high-resolution peaks of WS₂ and (E) XRD patterns of WS₂. Reproduced with permission from Van et al.⁹⁷ Copyright: 2021 Springer Nature. (F) Raman spectra of WS₂ and MoS₂. Reproduced with permission from Choudhary et al.⁹⁸ Copyright: 2016 Springer Nature.

phase with the semiconductor characteristics. In contrast, if the structure is octahedral so the 1T phase will be formed with metallic properties. The metallic phase 1T of MoS₂ and WS₂ was first discovered when MoS₂ or WS₂ was exfoliated by lithium intercalation into MoS₂ and WS₂ powder. Another rare phase of MoS₂ or WS₂ is 3R. The 3R phase can be described by three layers per unit

cell stacked with rhombohedral symmetry and trigonal prismatic coordination. It is difficult to prepare 3R phase of catalysts based on MoS₂ or WS₂. Therefore, very little work has been conducted on 3R phase of those materials. In Figure 14C,D, the bandgaps from the monolayer to the bulk WS₂ and MoS₂ are presented. In semiconductor materials, there are two separated energy

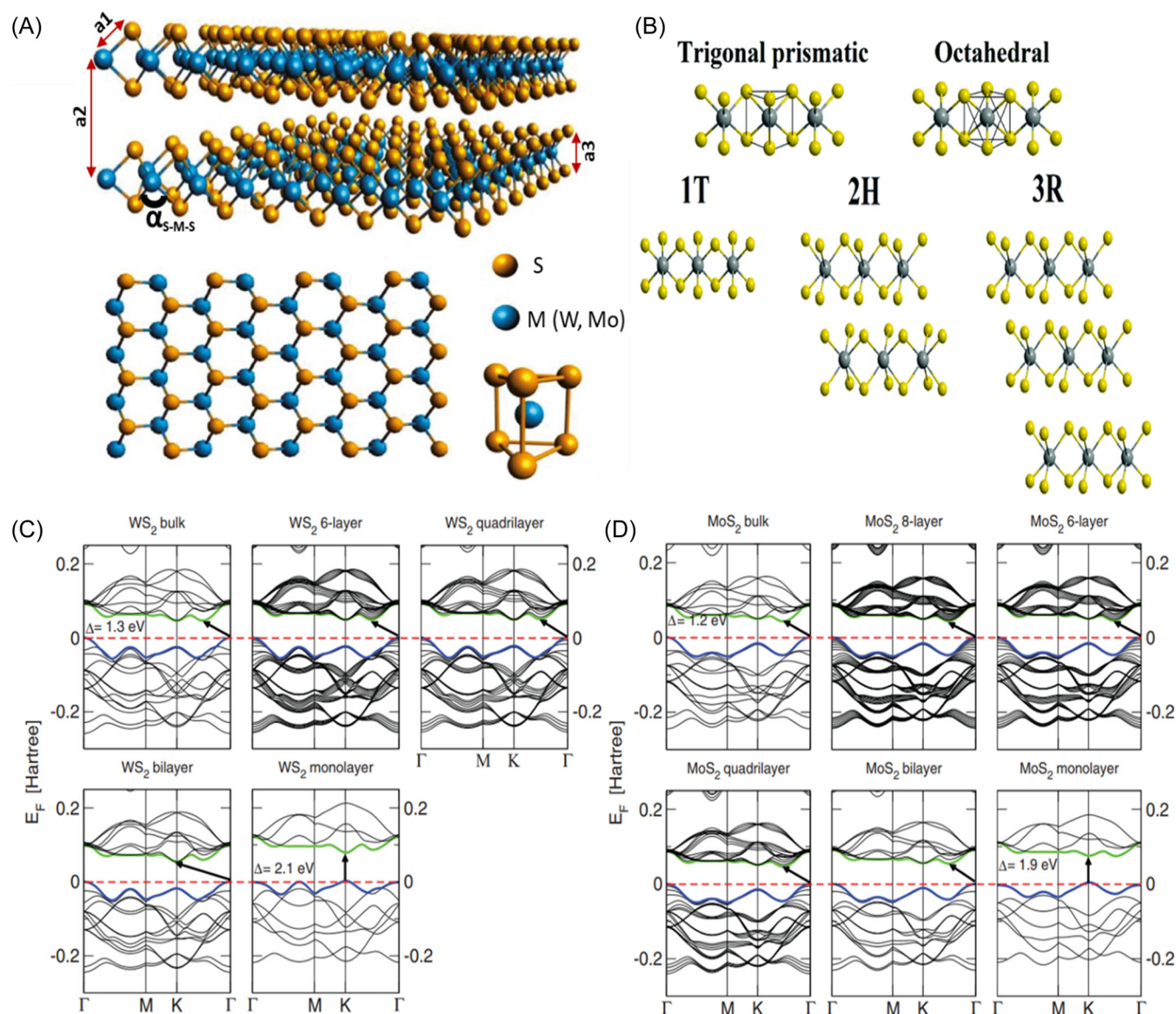


FIGURE 14 (A) Layered structure and top side view of WS₂ and MoS₂ structures. Reproduced with permission from Cotrufo et al.,¹⁰² Copyright: 2019 De Gruyter. (B) different phases of WS₂ and MoS₂ structures. Reproduced with permission from Coogan et al.,¹⁰³ Copyright: 2021 Royal Society of Chemistry. and (C, D) band structures of WS₂ and MoS₂. Reproduced with permission Kuc et al.¹⁰⁴ Copyright: 2011 American Physical Society.

TABLE 1 MoS₂ and WS₂ calculated structure

Catalysts	a_1 (Å)	a_2 (Å)	a_3 (Å)	E_b (meV atom ⁻¹)	E_g (eV)
MoS ₂	2.418	6.247	3.185	59.333	1.850
WS ₂	2.410	6.247	3.173	59.833	1.940

Note: The calculated structural parameters of MoS₂ and WS₂ with: a_1 , bond length of Mo-S and W-S; a_2 , $h_{\text{Mo-Mo}}$ and $h_{\text{W-W}}$ —vertical distance of two Mo atoms and two W atoms; a_3 , lattice constant of MoS₂ and WS₂; E_b , binding energies; and E_g , bandgap values.

area: valence band (VB) and conduction band (CB). The maximal energy of the valence band (VBM) and minimal energy of the conduction band (CBM) are characterized by a certain crystal momentum (K vector) in the Brillouin zone. If the K vectors are the same, the material has a

direct bandgap. In direct bandgap semiconductors, an electron can directly emit a photon. Otherwise, if the K vectors are different, the material shows the indirect bandgap. In the indirect band gap semiconductor, a photon cannot be emitted because the electron must

pass through an intermediate state and transfer momentum to the crystal lattice. It is clear that the multilayer or bulk materials of WS₂ and MoS₂ exhibit the indirect bandgap with different *K* vectors of VB and CB. In contrast, the monolayer of WS₂ and MoS₂ shows the direct bandgap with the same *K* vector of VB and CB. Therefore, numerous studies have investigated the properties as well as the catalytic activity of monolayer WS₂ and MoS₂. The bandgap of WS₂ material is from 1.30 to 2.1 eV and that of MoS₂ material is 1.2 to 1.9 eV depending on the number of layers of materials, where thinner catalysts lead to higher bandgap value. The calculated bandgap of WS₂ and MoS₂ from monolayer to bulk materials indicates that the number of layers of WS₂ and MoS₂ in materials significantly affects their physical properties, optical performance as well as the catalytic activity. Among them, monolayers with direct bandgaps show many advantages to optical technologies as well as catalytic applications.

The catalytic activities of electrocatalysts based on WS₂ and MoS₂ are highly affected by their layered structures. Therefore, the synthesis of monolayer and event metallic phases of WS₂ and MoS₂ by controllable processes and scalable and uniform catalysts is the main challenge to prepare effective catalysts for hydrogen technologies. In recent decades, significant achievements have been made to improve the performance of catalysts based on WS₂ and/or MoS₂ materials. However, the HER performance of WS₂ and/or MoS₂ and their derivatives still need to be enhanced for practical and commercial products. The following sections summarize the cutting edge of technologies as

well as the efficiency strategies that have been applied to prepare WS₂ and/or MoS₂ and their derivatives.

5 | PREPARATION OF MoS₂ AND WS₂ MATERIALS

5.1 | Atomic layer deposition

ALD is a cutting-edge technology for preparing catalyst materials. This is a new development from the chemical vapor deposition (CVD) technique. Using the ALD technique, a very thin film of catalysts can be deposited by the sequential use of a gas-phase chemical process. The principle of ALD reactions is to use two or more chemical elements as precursors. In the ALD process, on the functionalized substrate, one-by-one precursors will be deposited on and/or reacted with the surface of other layers deposited before. With precision timing and numbered layer control, a thin film is gradually formed with thickness control at Angstrom size and accurate composition of reactants. In recent years, considerable efforts have been devoted to the preparation of monolayers of MoS₂ and WS₂, which exhibit significant improvements in catalytic activity toward electrochemical processes. Therefore, with the high advantages, ALD has recently attracted considerable attention from researchers to fabricate different devices based on semiconductor materials, including thin films based on MoS₂ and WS₂, which could be employed for the HER process.^{105–107} The growth mechanism of the catalyst materials based on MoS₂ and WS₂ is shown in detail in Figure 15.

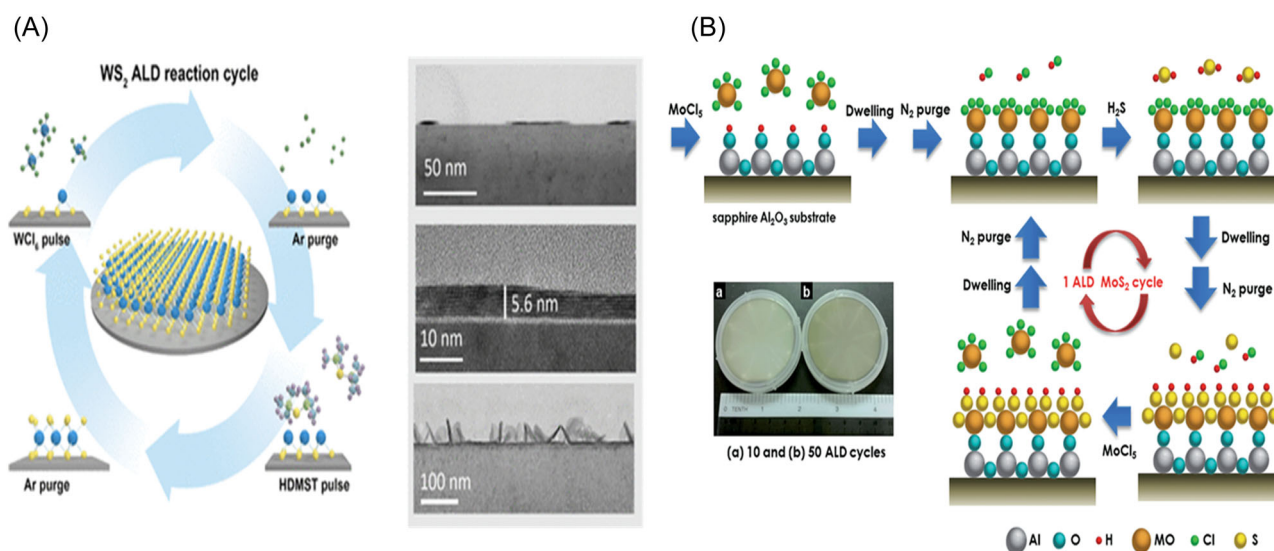


FIGURE 15 (A) Preparation schematic of ALD-grown WS₂ films. Reproduced with permission from Yang et al.,¹⁰⁸ Copyright: 2021 American Chemical Society. And (B) schematic showing the MoS₂ growth by the ALD route. Reproduced with permission from Tan et al.¹⁰⁹ Copyright: 2014 Royal Society of Chemistry. ALD, atomic layer deposition.

5.2 | Exfoliation from the bulk materials

In nature, MoS₂ and WS₂ are semiconducting materials normally found with 2H trigonal prismatic phases. The raw materials of MoS₂ and WS₂ exhibit poor conductivity and low catalytic active sites, which is challenging for the preparation of catalytic materials based on bulk MoS₂ and WS₂. Numerous studies have been conducted to boost the performance efficiency of catalysts based on these materials. Exfoliation is the very first and most effective route frequently used to overcome this obstacle. Using the exfoliation technique, the bulk materials are separated into thinner layers with 2–3 layers which propose a larger surface area and abundant active sites. Two popular techniques are often employed to exfoliate MoS₂ and WS₂ into layered catalysts: mechanical exfoliation and chemical exfoliation. Figure 16 shows

the exfoliation routes to prepare layered catalysts by using both mechanical and chemical exfoliation. Chemical exfoliation can be used to prepare monolayer or bilayer catalyst materials that exhibit high catalytic activities.^{110,111} Using chemical exfoliation, lithium, sodium, and potassium compounds have often been used to separate the layers of bulk catalysts.^{112,113} The insertion of cations into bulk catalysts could lead to some unique phenomena, such as the transformation of the 2H catalyst to 1T or 1T' materials, which exhibit better catalytic properties than primitive materials.^{114,115} Small-yield catalysts are sufficient for study but not for practical use or commercial materials. Recently, a second exfoliation technique, mechanical exfoliation, has been intensively investigated to prepare catalytic materials in larger quantities and with higher quality.^{110,116,117} Mechanical exfoliation has been significantly developed with noticeable results. However, chemical exfoliation still has some

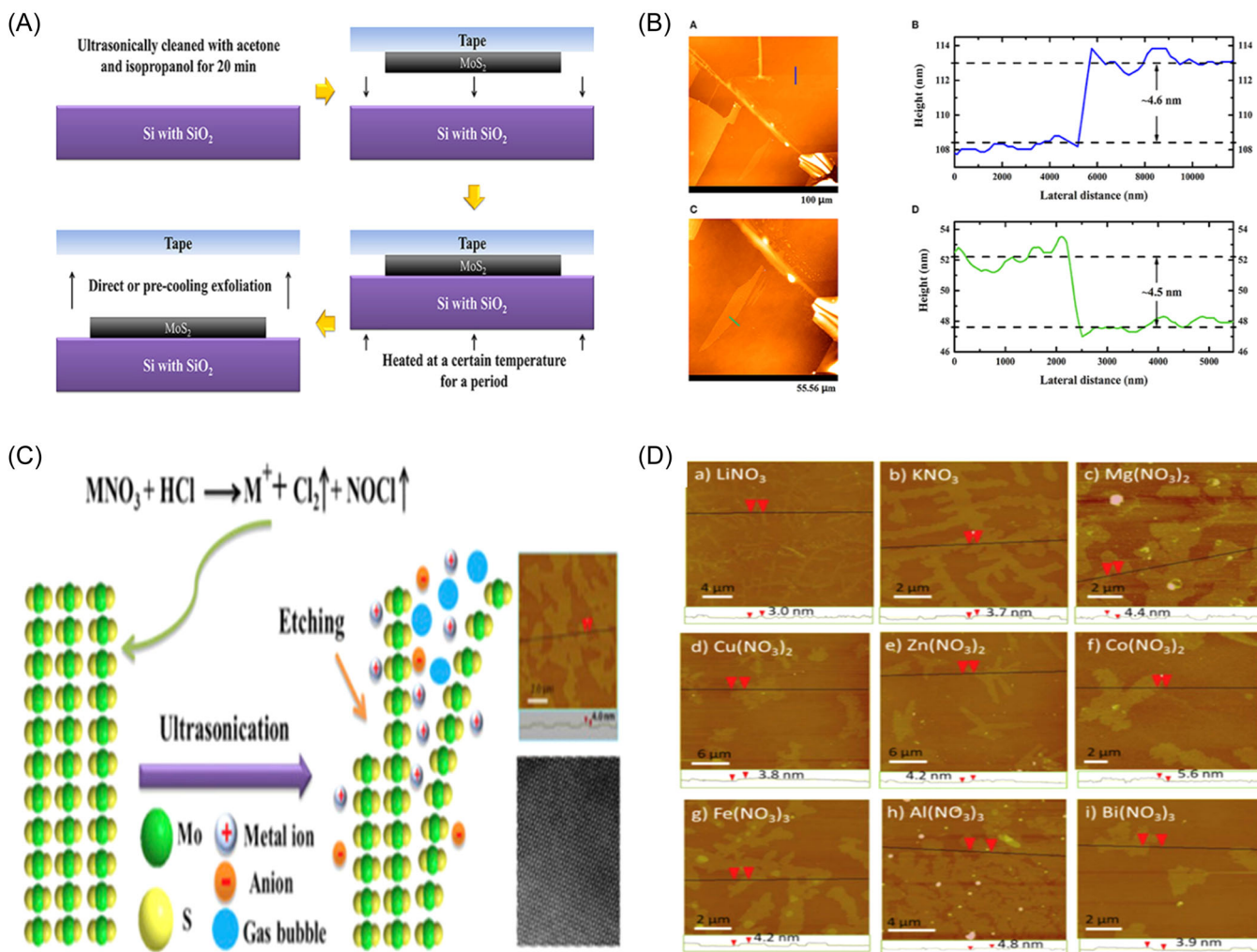


FIGURE 16 (A) Preparation of MoS₂ nanoflakes by thermal treatment and (B) atomic force microscopy (AFM) images of multilayer MoS₂ nanoflakes. Reproduced with permission from Zhang et al.,¹¹⁹ Copyright: 2021 Frontier Media S.A. (C) chemical exfoliation of MoS₂, and (D) various AFM images of the obtained MoS₂ nanosheets via chemical exfoliation in nitrate/HCl solutions. Reproduced with permission from Lin et al.¹²⁰ Copyright: 2017 Elsevier.

advantages over mechanical exfoliation which have been intensively studied by previous reports.^{114,115,118}

In summary, high-quality and layered 2D MoS₂ and WS₂ catalysts can be obtained by exfoliation of bulk materials via both mechanical and chemical routes. However, because of the time-consuming and difficult process control, as well as the small yield, the exfoliation technique faces difficulties in preparing practical catalytic materials.

5.3 | Hydro/solvothermal method

Hydrothermal and solvothermal methods are low cost, easy, and convenient for the large-scale synthesis of TMD-based nanomaterials. By changing one or more reaction conditions, such as the temperature, reaction time, type of metal precursors, surfactants, and/or solution reaction, the

synthesized products with different morphologies, phases, or crystallinity could be prepared. Because of all the above benefits, hydrothermal and solvothermal processes are considered as a convenient process to prepare nanostructured materials.^{121,122} Recently, MoS₂ and WS₂ have been intensively prepared by hydrothermal reactions to investigate their HER performances. Various morphologies, structures, and new materials have been prepared by changing one or more reaction conditions of the synthesis process as shown in Figure 17. Heterostructures of MoS₂ and WS₂ with other catalysts or MoS₂/WS₂ heterostructures could also be prepared using these methods.^{123–126}

Generally, because of the controllable and large-scale process with different catalysts, hydrothermal and solvothermal techniques can be used to prepare various catalyst materials based on MoS₂ and WS₂ for electrochemical applications, including the HER, batteries, and supercapacitors.

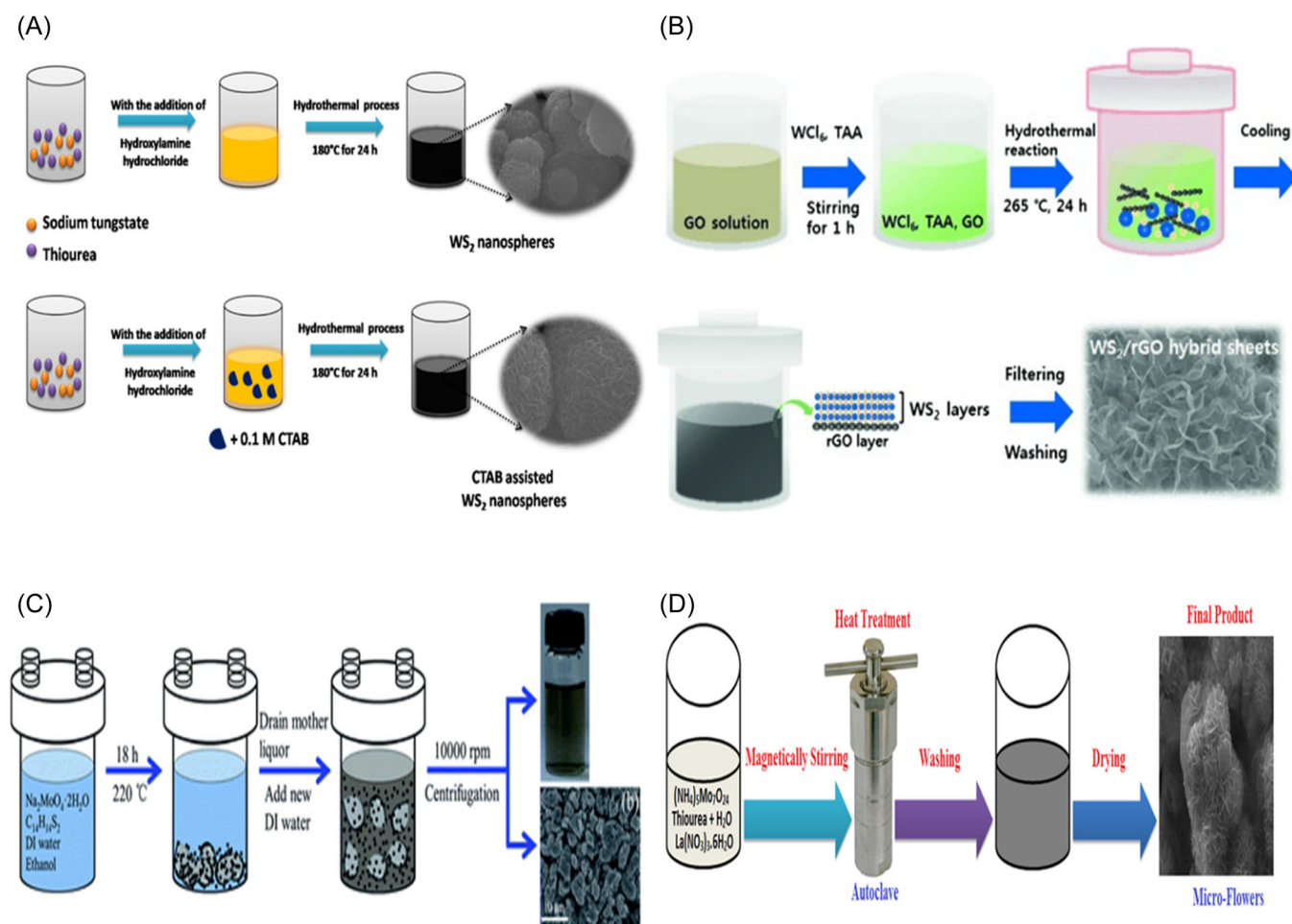


FIGURE 17 (A) Synthesis of WS₂ and CTAB-assisted WS₂ nanostructures. Reproduced with permission from Swathi et al.,¹²⁷ Copyright: 2021 Elsevier. (B) synthesis of WS₂/rGO hybrid sheets by the hydrothermal reaction. Reproduced with permission from Yang et al.,¹²⁸ Copyright: 2013 John Wiley and Sons. (C) the preparation of MoS₂ QDs using a hydrothermal method. Reproduced with permission from Ren et al.,¹²⁹ Copyright: 2015 Royal Society of Chemistry. And (D) synthesis of MoS₂ nanoflower using hydrothermal route. Reproduced with permission from Nadeem Riaz et al.¹³⁰ Copyright: 2018 John Wiley and Sons. CTAB, cetyltrimethyl ammonium bromide; DI, deionization; QD, quantum dot; rGO, reduced graphene oxide; TAA, thioacetamide.

5.4 | Chemical vapor deposition

CVD is a vacuum deposition method that is typically employed to prepare catalyst electrodes for thin films. A high-quality thin-film catalyst could be formed by a chemical reaction on the surface of substrates such as silicone or p-type silicone using one or more gaseous resources such as N_2 or CH_4 and/or elemental substances containing thin-film elements. The CVD route has various advantages to prepare catalyst thin films such as high-quality film, low-defect, and exactly controllable thickness of catalyst film on substrates. One of the advances in vapor-phase deposition involves the adjustment of the precursor ratio. The exact time and temperature of the components

can be easily controlled, and well-contacted interfaces between nanostructures and substrates are favorable for charge migration. Additionally, high-quality catalysts obtained via the CVD method also provide a simple but pure platform to investigate the HER mechanism. In a typical CVD synthesis process, Mo or W is placed in the furnace at the center of the heating zone, while S powder is placed upstream relative to the flow direction of the carrier gas (Ar or N_2). When the temperature increases, the S vapor flows downstream, converting the Mo or W precursor into MoS_2 or WS_2 in the high-temperature zone. Figure 18A,B shows the synthesis of MoS_2 and WS_2 , respectively, by the CVD technique. The preparation of high-quality catalysts based on MoS_2 or WS_2 via CVD

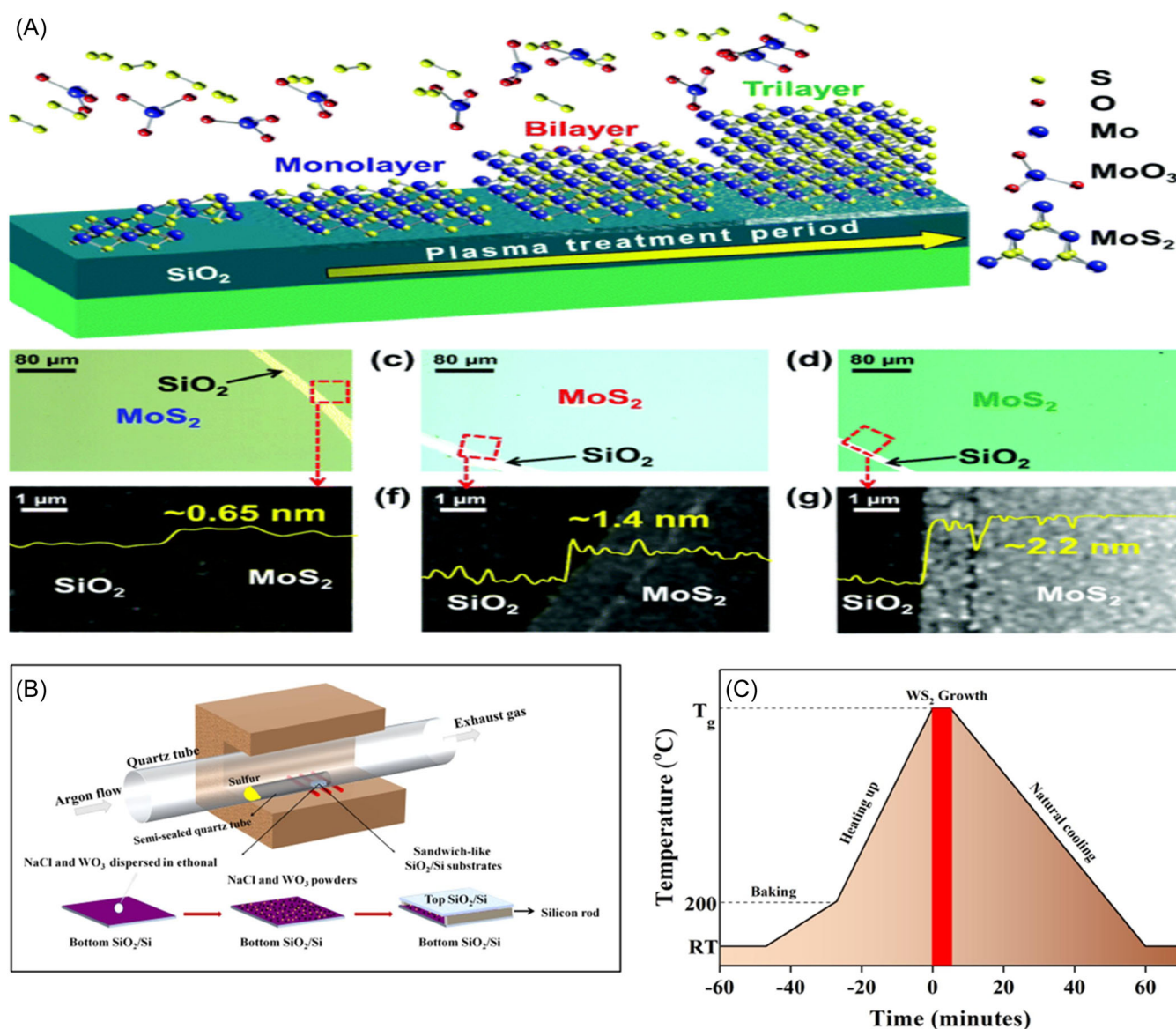


FIGURE 18 (A) Preparation of MoS_2 thin film by chemical vapor deposition (CVD) method. Reproduced with permission from Jeon et al.,¹³¹ Copyright: 2015 Royal Society of Chemistry. (B) preparation of WS_2 thin film by CVD method, and (C) time management for the synthesis of catalysts by the CVD technique. Reproduced with permission from Shi et al.¹³² Copyright: 2020 Elsevier.

requires careful modulation of important parameters. The temperature is the most important parameter that must be checked for each process. The distance between the S powder and the Mo or W source is also a critical factor to prepare high-quality thin films. Another important factor is the flow of the carrier gas, usually Ar or N₂, which needs to be controlled precisely so that the S powder can be properly deposited on the substrates where the Mo or W source is placed. In addition, the reaction time for different states must be adjusted correctly to form the highest-quality catalyst, as shown in Figure 18C.

5.5 | Other synthetic processes

In addition to the methods mentioned above, other synthetic pathways have also been used to fabricate catalysts based on MoS₂ and WS₂ materials. Thermal annealing is a straightforward method for preparing MoS₂- and WS₂-based materials. However, it is difficult to obtain MoS₂ or WS₂ with a well-controlled morphology and a number of layers. Moreover, high temperatures may often lead to material aggregation, which limits the HER performance. Even so, research attention has been paid to this method for obtaining electrocatalysts with decent HER catalytic activity. Chemical vapor transport (CVT) is typically utilized to obtain high-quality bulk single crystals. In this technique, raw materials react with transport agents, usually pure halogen elements or their compounds, in the hot zone, and are then transported to the cold zone, where the growth of single crystals is observed. The growth temperature, transport agent, and reaction time are the main parameters that should be carefully tuned to obtain high-quality MoS₂ and WS₂ single crystals. Sputtering is another effective method for preparing high-quality catalysts based on MoS₂ and WS₂. Owing to the high purity of the as-grown films, these samples are also suitable for investigating the origin of the catalytic activities. Figure 19A,B shows the synthesis of catalysts by the CVT and sputtering methods, respectively. In addition, electrodeposition is also an effective route to prepare highly pure MoS₂ and WS₂ catalysts for HER applications, as shown in Figure 19C, which were also reported in detail by previous reports.^{133,134}

6 | ENGINEERING STRUCTURE OF CATALYSTS BASED ON MoS₂ AND WS₂ TO ENHANCE HER ACTIVITY

The electrocatalytic activities of MoS₂ and WS₂ are much more efficient than those of TMDs and other materials, except for the Pt material group. However, to prepare

practical and commercial materials, particularly at the industrial scale, the catalytic characteristics of catalysts based on MoS₂ and WS₂ require further investigation and improvements. In numerous studies, the catalytic activities of catalysts based on MoS₂ and WS₂ have been significantly improved by different techniques and methods, as listed below.

1. Improving the active surface of prepared catalysts.
2. Doping with other elements to boost catalytic activity.
3. Modifying the structure or morphology of catalysts.
4. Preparing heterostructure materials with other materials.

A detailed explanation, interpretation of research, and examples are provided to clearly understand each strategy as below.

6.1 | Preparing catalysts with larger active surface

As typical 2D catalysts, MoS₂ and WS₂ have a layered structure in which the catalyst layers can be stacked together by vdW forces. Although 2D catalysts exhibit large specific surface area, however, the poor conductivity and inactive basal planes could greatly hinder the HER process. In theory, the catalytic activity of 2D catalysts is basically located at the edge sites and defects of material. For the electrocatalytic process, the catalysts active area is one of the most crucial factors which could highly affect the kinetic and rate of process. Therefore, many strategies have been usually employed to elevate the active sites of catalysts surface which could be categorized into two common classes including increase of active site on catalyst edge and modifying the basal planes of catalysts. The first one is engineering the catalyst structure to increase the active sites which are considered as the edges of MoS₂ and WS₂ layers. To achieve that goal, two approaches are often employed including synthesis catalysts with the increase of edge length or preparing monolayer catalysts. In fact, to increase the edge length of catalysts, that means the size of catalysts also have to be lengthened, it is a really big challenge in nanoscience. Along with that, to prepare monolayer catalysts, there are also many drawbacks such as small yield and time consumption as we discussed in the above section. To date, modifying the structure of catalysts based on MoS₂ and WS₂ has been intensively studied to increase their catalytic activity. Different techniques have been applied to prepare various effective catalysts with a larger active surface. Among them, hollow structure and smaller size of catalysts are the

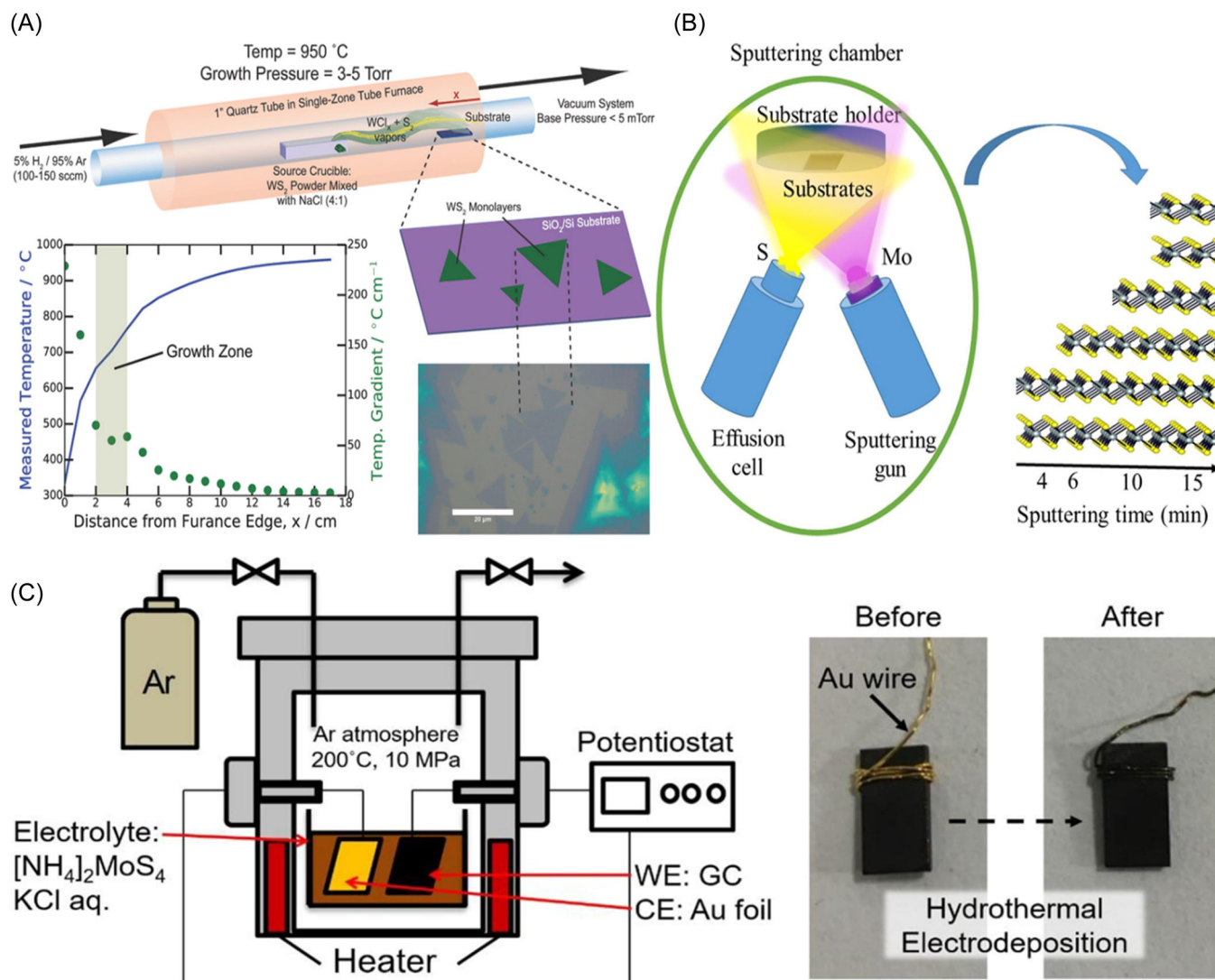


FIGURE 19 (A) Synthesis of WS₂ by chemical vapor transport. Reproduced with permission from Modtland et al.,¹³⁵ Copyright: 2017 John Wiley and Sons. (B) synthesis of MoS₂ by the sputtering method. Reproduced with permission from Rigi et al.,¹³⁶ Copyright: 2020 Elsevier. And (C) preparation of MoS₂ electrocatalysts by electrodeposition. Reproduced with permission from Nakayasu et al.¹³⁷ Copyright: 2022 Elsevier. CE, counter electrode; GC, glassy carbon; WE, working electrode.

prominent materials to improve HER efficiency as shown in Figure 20.

The second strategy is also investigated to prepare effective catalysts in which the basal planes of MoS₂ and WS₂ will be reconstructed to prepare dangling bond on that. It is clear that, the dangling bond states closer to the Fermi level (E_F), which activates the basal plane for HER. In fact, the basal planes of MoS₂ and WS₂ exhibit very low catalytic activity because of poor electron transport properties between layers. Therefore, many studies have been investigated to improve the catalytic activity of large inert basal planes by creating the defects. With structural defects on basal planes, the local electron density could be induced and that could increase the HER process by modulating the electronic structures of prepared catalysts. For instance,

DFT results indicate that increasing the S atom vacancies (S-vacancies) could strengthen hydrogen adsorption and strain the S-vacancy sites, which would lead to an optimal ΔG_{H^*} and make the gap states close to the E_F .¹⁴⁰⁻¹⁴² However, defect density must be controlled to avoid excess defects which could harm the catalytic activity of catalysts. In the last decades, various techniques, such as plasma treatment or chemical functionalization, have been used to increase the defect density of both MoS₂ and WS₂ catalysts. As shown in Figure 21A, after treatment with O₂ and H₂, the catalytic activity of MoS₂ is significantly improved. As shown in Figure 21B, annealing in a H₂ atmosphere could prepare a catalyst with defects based on WS₂ surface, which also shows a significant improvement in the HER performance.

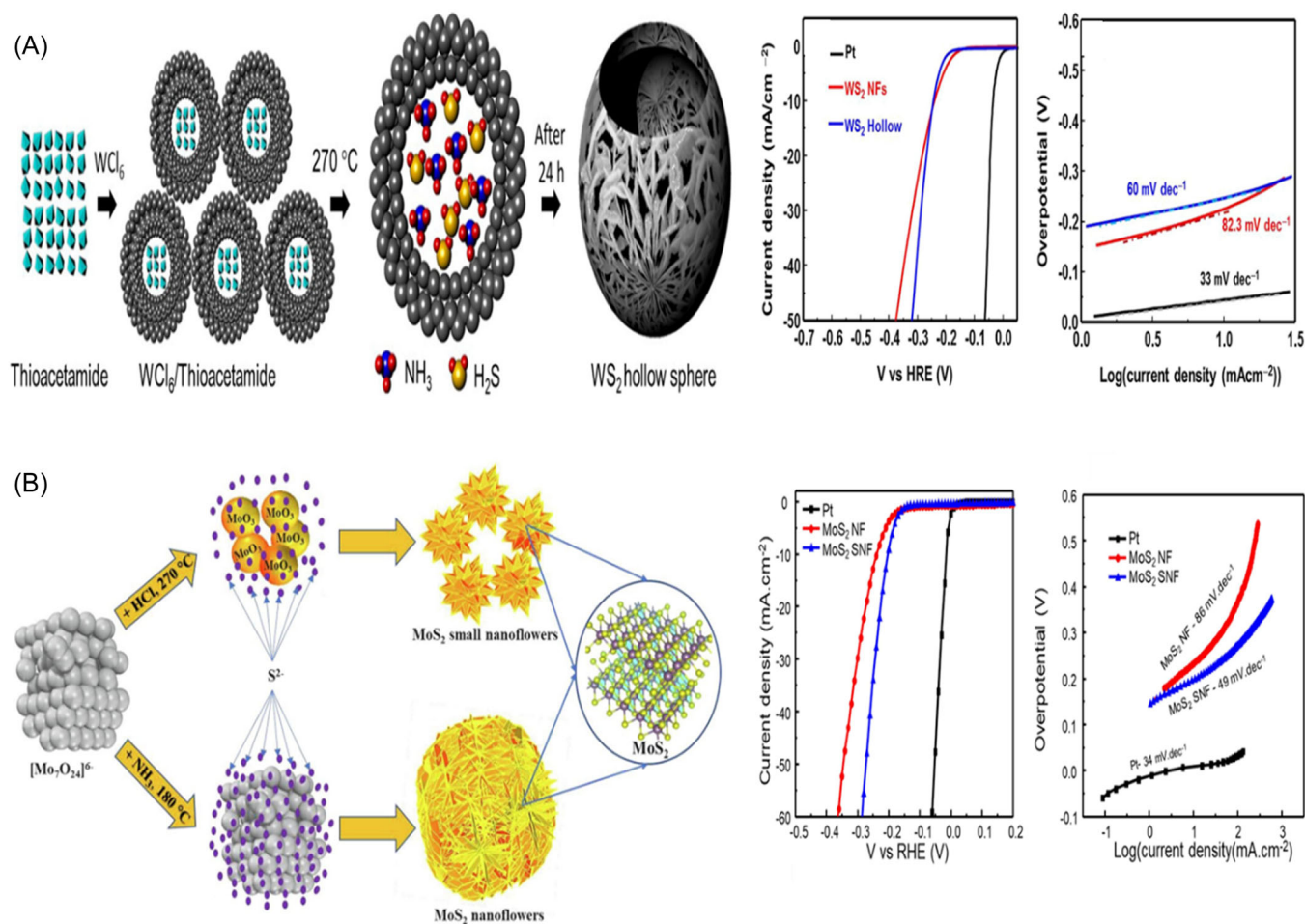


FIGURE 20 (A) Synthesis of WS_2 hollow spheres. Reproduced with permission from Nguyen et al.,¹³⁸ Copyright: 2020 Elsevier. And (B) synthesis of super small MoS_2 nanoflowers. Reproduced with permission from Van Nguyen et al.¹³⁹ Copyright: 2023 Elsevier. NF, nanoflower; SNF, small nanoflower.

6.2 | Heteroatom doping

By adding a small amount of other elements to the layered MoS_2 and WS_2 , their electrocatalytic performance dramatically increases. As mentioned in the Volcano plot, the material with appropriate HBE which is not too weak nor too strong is a desirable catalyst for HER application. In those materials, the adsorption free energy of H^* (ΔG_{H^*}) is closed to the Volcano peak like Pt group. With $\Delta G_{\text{H}^*} \approx 0$, the intermediate hydrogen elements could be easily absorbed and desorbed into/from electrode surface because of the rapid proton/electron transfer between electrolyte and cathode. Therefore, the HER performance could be dramatically improved. Many studies have indicated that doping with very small concentrations of noble metal into MoS_2 and WS_2 catalysts could be the effective route to boost the catalytic activity of doped materials. The electronic interactivity among different atoms plays the role of modifying the electron structure of MoS_2 and WS_2 , especially, in which Mo and W are the d-band materials. The doped strategy could be grouped into two types of doped catalysts

which are metal-doped catalysts and nonmetal-doped catalysts. Both routes have their own advantages and drawbacks as well as we have to choose the suitable doping elements for each host catalyst due to their different effects on the HER activity.

In metal doping methods, several metals such as Pt, Au, Co, Ni, and Cu have already been usually utilized as great doping elements into MoS_2 and WS_2 materials. Figure 22 shows the results of HER performance of various elements doped in MoS_2 and WS_2 . In Figure 22A, Pd-doped WS_2 exhibits a significant increase toward HER application with a Tafel slope of 54 mV dec^{-1} and an overpotential of -175 mV at -10 mA cm^{-2} . On the other hand, Figure 22B shows the remarkable catalytic activity of Zn-doped MoS_2 compared with that of other doping metals with the onset potential of -0.13 V versus reversible hydrogen electrode and the Tafel slope of 51 mV dec^{-1} . The significant improvement is considered to be the energy band alignment near the H^+/H_2 reduction potential which could reduce ΔG_{H^*} and increase the density of the active sites as well as the improving conductivity.

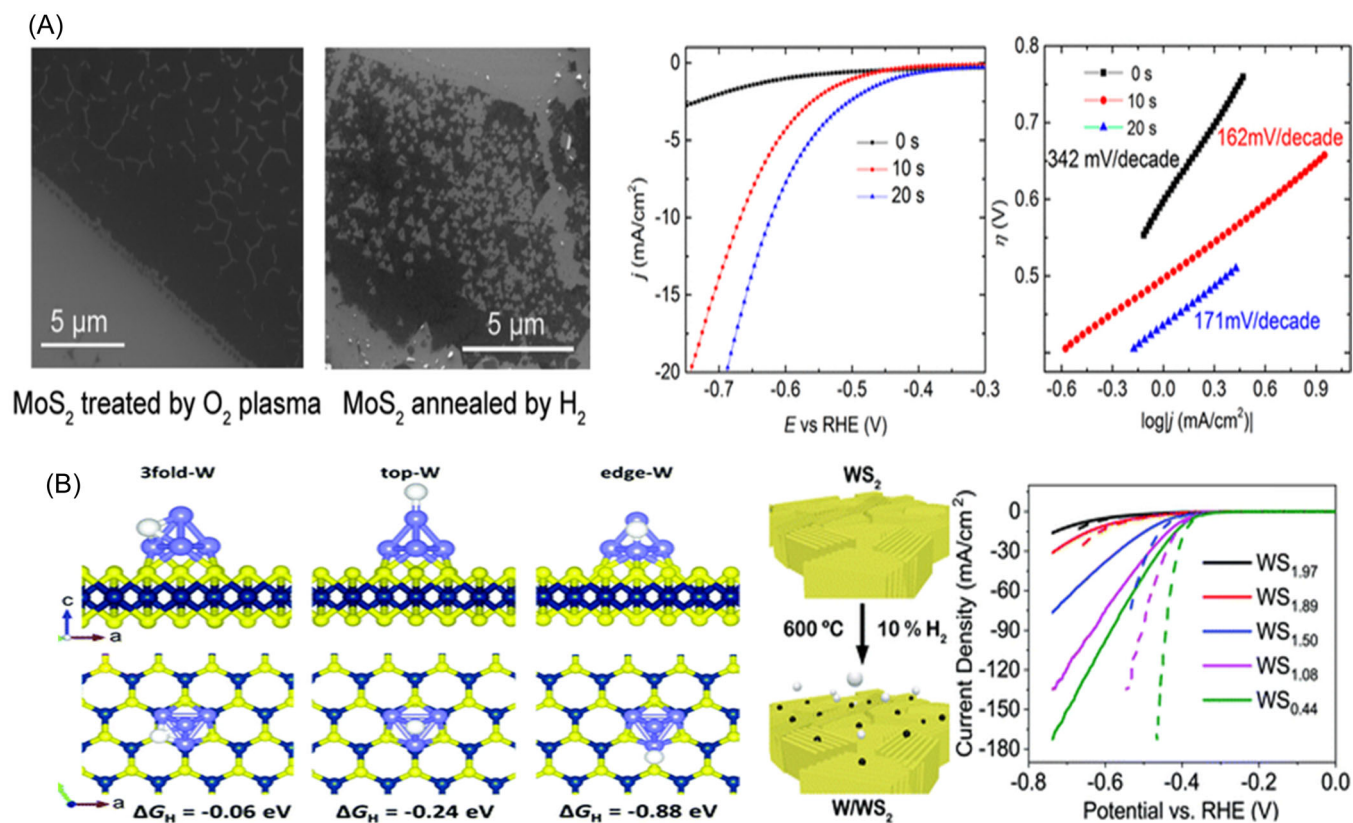


FIGURE 21 (A) Defect-engineered monolayer MoS₂ for improved hydrogen evolution reaction (HER). Reproduced with permission from Ye et al.,¹⁴³ Copyright: 2016 American Chemical Society. and (B) improving the HER performance of 2H-WS₂ by defect engineering. Reproduced with permission from Wu et al.¹⁴⁴ Copyright: 2019 Royal Society of Chemistry. RHE, reference hydrogen electrode.

For the nonmetal doping process, nitrogen and phosphorus elements have been intensively investigated using various techniques. The improvement of catalytic activity toward HER application of catalysts based on N or P doped into MoS₂ and WS₂ is illustrated in Figure 23. In the structure of catalysts based on nonmetal-doped MoS₂ or WS₂, there are different effects of doped elements onto host elements. At first, they could create the disorder structure of catalysts which is caused to increase the number of active sites in HER catalysts. Therefore, more active sites could be generated in doped catalysts. Second, based on the disorder of synthesized materials, the doped catalysts with higher carrier concentration could be prepared as well as the electronic structure of doped catalyst could be tunable. Therefore, the intrinsic conductivity of catalysts could be controllably enhanced and significantly improve after the doping process. On the basis of this principle, Xie et al. conducted the experiment to incorporate oxygen with MoS₂.¹⁴⁷ The performance of O-doped catalysts is highly impressive with a current density of 126.5 mA cm⁻² at an overpotential of 300 mV, a low onset overpotential of 120 mV, a small Tafel slope of 55 mV dec⁻¹. The excellent long-term stability is also achieved. The results indicate that the catalyst based on optimized O-doped MoS₂ could

be a great material for HER application which could be considered as an alternative for Pt metal.

6.3 | Phase engineering

MoS₂ and WS₂ exhibit multiple crystal phases, as mentioned above. Normally, MoS₂ and WS₂ exist in nature as the 2H phase, which corresponds to a semiconductor, and those materials are often employed to prepare different catalysts based on MoS₂ and WS₂. In contrast, the 1T and 1T' phases of MoS₂ and WS₂ have more catalytic advantages, including the larger density of the active sites, metallic conductivity, and better electrode kinetics. Therefore, the 1T and 1T' phases of MoS₂ and WS₂ show higher catalytic activities than those of the 2H phases. Because of the superior catalytic activity, numerous studies have been devoted to transform to prepare 1T and/or 1T' phase of MoS₂ and WS₂ from the nature phase of materials. In Figure 24A, the free energy for HER of Mo atoms of 2H and 1T phases was calculated. We can see a significant decrease in free energy of the 1T phase compared with that of the 2H phase. In Figure 24B, the HER performance of different phases of catalysts based on WS₂ was investigated. It is clear that the metallic 1T

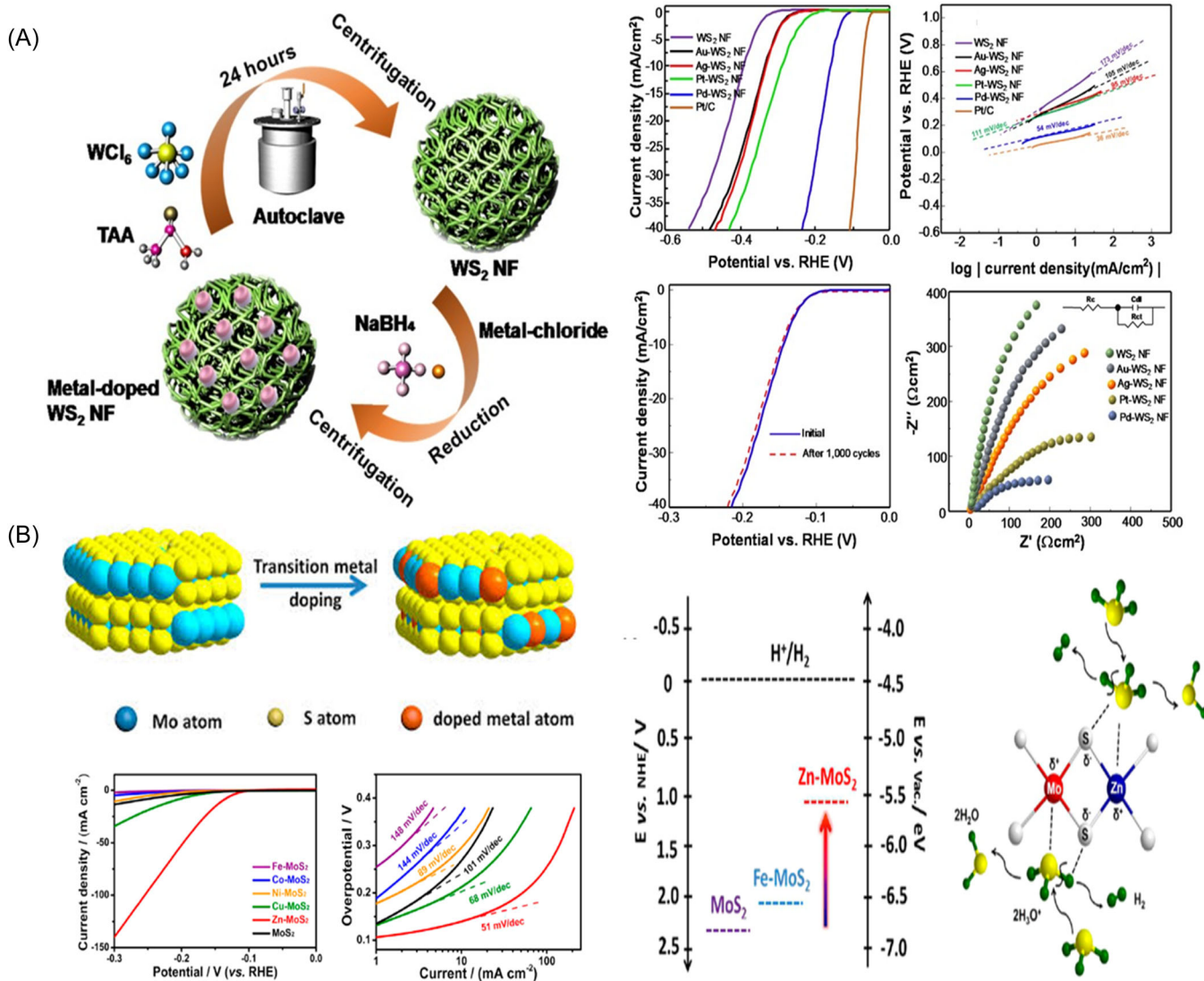


FIGURE 22 (A) Doping different metals on WS₂. Reproduced with permission from Hasani et al.,¹⁴⁵ Copyright: 2018 Elsevier. And (B) transition-metal doping on MoS₂. Reproduced with permission from Shi et al.¹⁴⁶ Copyright: 2017 American Chemical Society. NF, nanoflower; PVC, polyvinyl chloride; TAA, thioacetamide.

phase of WS₂ exhibits a much better HER performance than those of the performance of the 2H phase. This enhancement in catalytic activity is caused by the increased number of active sites on MoS₂ and WS₂ at the edges sites as well as the metallic properties of polymorph in the 1T phase. Chemical exfoliation route is often employed to obtain single- or few-layered 1T/1T' MoS₂ and WS₂.^{152,153} In which, lithium intercalation is the main mechanism to prepare layers catalysts. Element doping, heat treatment, or electrochemical treatment could be conducted to engineer the 2H phase into the 1T/1T' phase of MoS₂ and WS₂.^{154,155} For instance, if 2H MoS₂ is treated by an electrochemical process, the 2H phase will be partially transformed into 1T phase to form in-plane 1T-2H MoS₂ hybrid phase. The 2H/1T hybrid phase enhances structural disorder and electronic

conductivity as well as it causes the decrease of hydrogen adsorption-free energy. Compared with the initial phase of 2H-MoS₂, the hybrid-phase MoS₂ electrocatalyst exhibits remarkably improved HER activity with a lower onset overpotential and Tafel plot. Specifically, the overpotential and Tafel plot of the electrochemically treated MoS₂ nanosheets were decreased, respectively, by 174 mV and 25 mV dec⁻¹ at a cathodic current density of 10 mA cm⁻² compared with pristine 2H-MoS₂ nanosheets. This significant improvement is assigned to the electrochemical treatments which synergistically modulate both the structural and electronic properties of multilayer 2H-MoS₂ nanosheets.¹⁵⁶

In many previous studies, most experimental results confirmed that the 2H phase of MoS₂ and WS₂ cannot be totally changed into the 1T phase. They indicated that

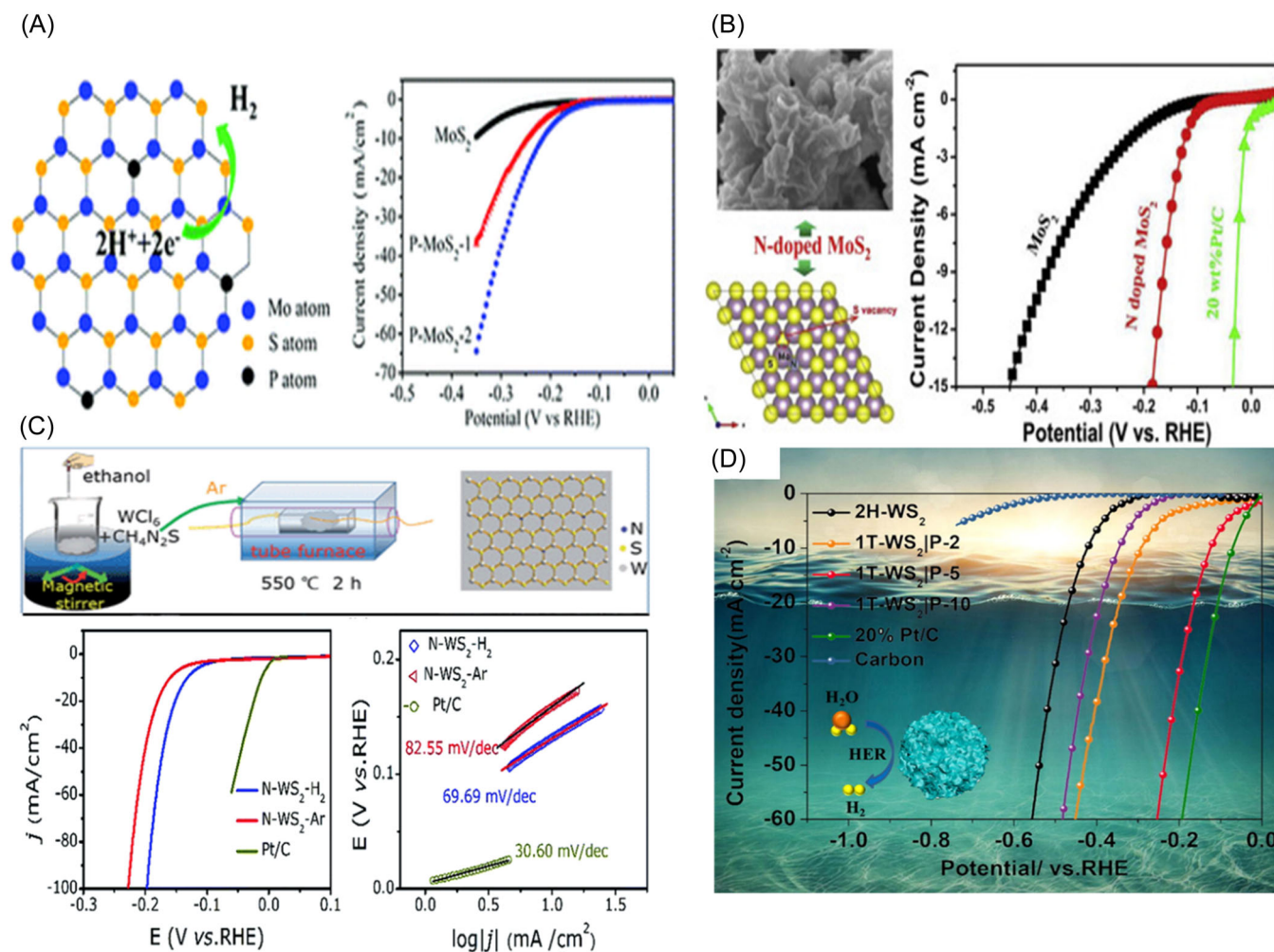


FIGURE 23 (A) The hydrogen evolution reaction (HER) performance of P-doped MoS₂. Reproduced with permission from Ren et al.,¹⁴⁸ Copyright: 2020 Royal Society of Chemistry. (B) the HER performance of N-doped MoS₂. Reproduced with permission from Li et al.,¹⁴⁹ Copyright: 2017 Elsevier. (C) the HER performance of N-doped WS₂. Reproduced with permission from Sun et al.,¹⁵⁰ Copyright: 2016 Royal Society of Chemistry. And (D) the HER performance of P-doped WS₂. Reproduced with permission from Sun et al.¹⁵¹ Copyright: 2022 Elsevier. RHE, reference hydrogen electrode.

there is maybe around 20% of the initial phase leftover after the process. That is why the obtained materials are usually mixed 1T and 2H phases. Another drawback of this method is the poor stability of the 1T phases of MoS₂ and WS₂. Along with the working time, catalysts based on the 1T phase of MoS₂ and WS₂ can be easily converted back into the 2H phase, causing a quick collapse in HER performance. In fact, synthesis of electrocatalysts for the HER process under high temperatures by hydrothermal/solvothermal techniques or CVD, the 2H phase of MoS₂ and WS₂ catalysts is usually formed. However, along with the development of technologies and numerous efforts of scientists, the metallic phases 1T or 1T' of MoS₂ and WS₂ have also been easily prepared by a conventional process. Nevertheless, it is difficult to control the process, uniformity, and purity of the catalysts phase. More importantly, the catalytic performance, including the

lifetime of electrodes based on 1T or 1T' phases of MoS₂ and WS₂, still needs to be further improved.

6.4 | Synthesis hybrid/composites catalysts

In the HER process, the reaction on the surface of electrodes highly depends on the effective interaction between the catalysts and hydrogen elements in the electrolyte. In the last decades, many effective hybrid catalysts based on MoS₂ and WS₂ have been reported as great materials for the HER process. Hybrid catalysts could present many distinct improvements because they have various advantages, including synergistic effects as well as strain effects and electronic interactions. In fact, MoS₂ and WS₂ could be combined with various types of materials to create different

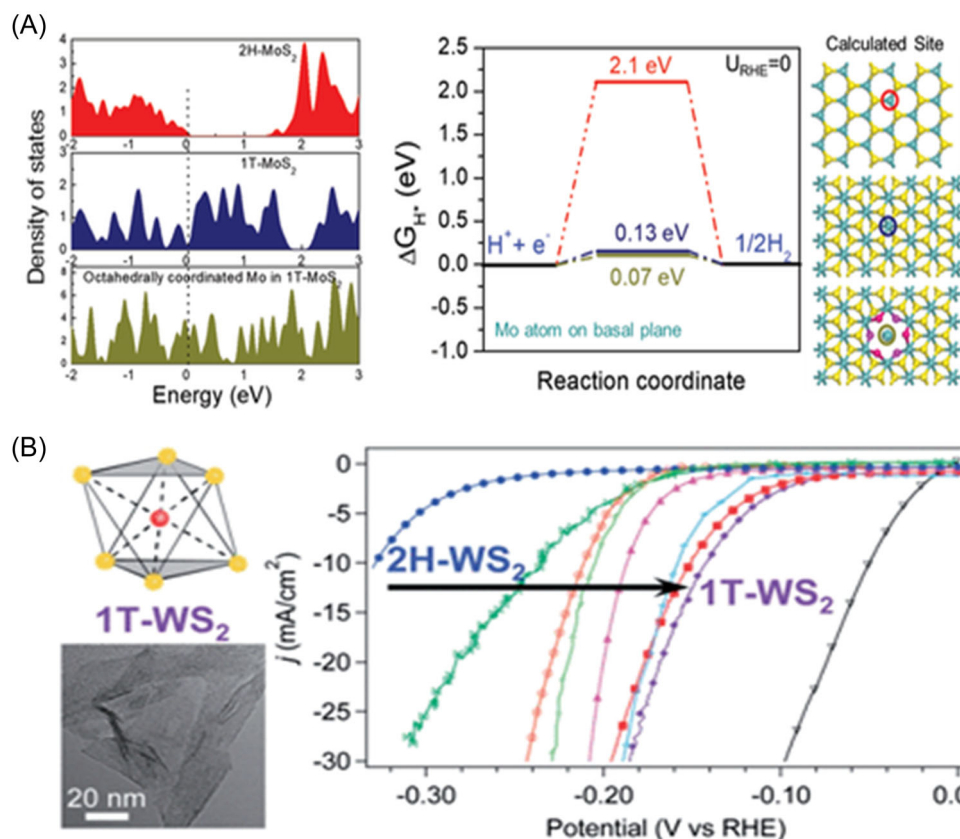


FIGURE 24 (A) The free-energy diagram for hydrogen evolution reaction (HER) of different phases of MoS₂. Reproduced with permission from Zhang et al.,¹⁵⁷ Copyright: 2019 John Wiley and Sons. And (B) HER performance of 1T and 2H phases of WS₂. Reproduced with permission from Lukowski et al.¹⁵⁸ Copyright: 2014 Royal Society of Chemistry. RHE, reference hydrogen electrode.

catalysts that can boost the HER performance. The hybrid catalysts based on MoS₂ and WS₂ can be classified into two main types. First, MoS₂ and WS₂ can be integrated with graphene or reduced graphene to create conductivity platforms for catalyst materials, as indicated in Figure 25. In these synthesized catalysts, the conductivity and the active site of the hybrid catalyst could be significantly improved by the effect of graphene layer as a conductive platform. In this heterostructure material, the carrier migration efficiency of MoS₂ and WS₂ can be accelerated, and the intrinsic catalytic activity can also be significantly increased.

Another hybrid material of catalysts based on MoS₂ and WS₂ is the heterostructure of MoS₂ and WS₂ with other catalysts, such as NiS₂, CoS₂, or MoO₃. In these hybrid materials, the synergistic effect and electronic interaction of different catalysts are the main reason for the improvements in catalytic activity. In semiconductor physics theory, one of the important roles of heterostructure is the boost of the directional migration of electrons with properly matched band structures in different catalysts. The synergistic effect between different material phases has also been investigated in previously reported. For example, in the incorporated catalysts of Co/MoS₂, the 3D isosurface indicates that coupling of Co with MoS₂ produces the redistribution of

electron density, and the electron transfer occurs from Co to MoS₂ in the interfacial region.¹⁶¹ The electron depletion on Co moiety and electron accumulation on the MoS₂ side is believed to strengthen the activation of H₂O molecule and expedite the electron-transfer process in the Volmer and Heyrovsky steps, thus leading to the significantly enhanced electrocatalytic activities. The Gibbs free energy of water adsorption (ΔG_{H_2O}) is generally considered as a vital parameter of the rate-limiting Volmer step in alkaline conditions. The DFT calculation shows that the (ΔG_{H_2O}) on Co/MoS₂ is calculated to be -1.69 eV, which is drastically lower than that of MoS₂ (-0.21 eV). Other hybrid catalysts with catalytic improvement results are shown in Figure 26. It can be seen that the HER performance of prepared heterostructure catalysts is significantly improved compared with that of pristine MoS₂ or WS₂.

7 | CONCLUSION AND PERSPECTIVES

Over the last decades, MoS₂ and WS₂ have been intensively investigated and employed for energy storage and electrochemical applications because of their

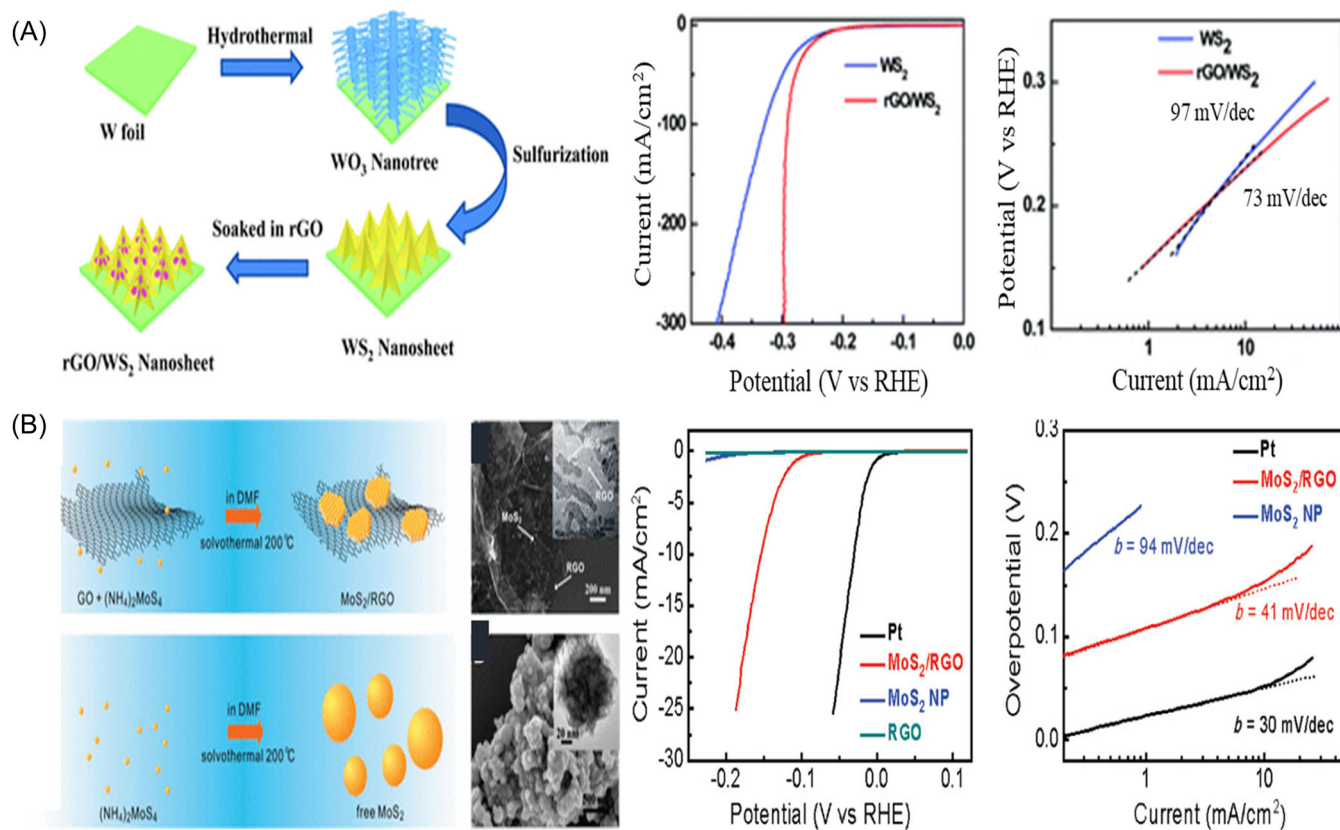


FIGURE 25 (A) WS₂ nanosheet sensitized by graphene. Reproduced with permission from Shifa et al.,¹⁵⁹ Copyright: 2015 Royal Society of Chemistry. And (B) MoS₂ nanoparticles grown on graphene for the hydrogen evolution reaction. Reproduced with permission from Li et al.¹⁶⁰ Copyright: 2011 American Chemical Society. NP, nano particle; rGO, reduced graphene oxide; RHE, reference hydrogen electrode.

abundant natural resources, low prices, low toxicity, and superior catalytic activity. The properties of MoS₂ and WS₂ are greatly affected by the size and electronic charge of transition metals, which causes various unique characteristics and the improved performance of the catalysts. Numerous effective approaches have been carried out to improve the electrocatalytic performance of catalysts based on MoS₂ and WS₂ materials. In this review, we briefly summarized the HER mechanism and its crucial parameters. The structure and properties of MoS₂ and WS₂ are also compared in detail. Besides that, the recent advances of catalysts based on MoS₂ and WS₂ materials for HER have been addressed.

MoS₂ is considered the most promising catalyst for HER applications after Pt-based catalysts. The ideal structure and Pt-like performance toward the HER are the key advantages of MoS₂ compared with other catalytic materials. Besides that, WS₂ has also been intensively investigated and considered a great candidate for HER applications on a practical scale because its structure and catalytic activities are highly comparable to that of MoS₂. The layered 2D structure of MoS₂ and WS₂ leads to different special chemical and physical characteristics which are greatly

beneficial for the HER process. Therefore, both MoS₂ and WS₂ could be considered as the prominent materials for catalytic applications which could be replaced for Pt group metals to prepared working electrode in electrochemical process. Significant efforts have been devoted to developing the efficiency as well as economic aspects of electrocatalyst materials based on MoS₂ and WS₂ for hydrogen energy technologies. Along with the significant developments of high technologies, the HER performances of these catalysts have been dramatically improved. However, it still remains a big challenge to prepare large-scale, high-quality, and commercial electrodes based on MoS₂ and WS₂ to produce hydrogen gas. Besides that, the synthesis process reactions of catalysts based on MoS₂ and WS₂, as well as the mechanism of the HER application using MoS₂ and WS₂, are not fully understood. So far, most studies have reported a simple combination of MoS₂ and WS₂ with doping elements and heterostructures with other materials. These improvements have not been appropriate for practical requirements. It is clear that a large research gap needs to be filled to increase the catalytic activity of catalysts based on MoS₂ or WS₂ materials. In fact, considerable efforts have been devoted as well as different strategies, methods and

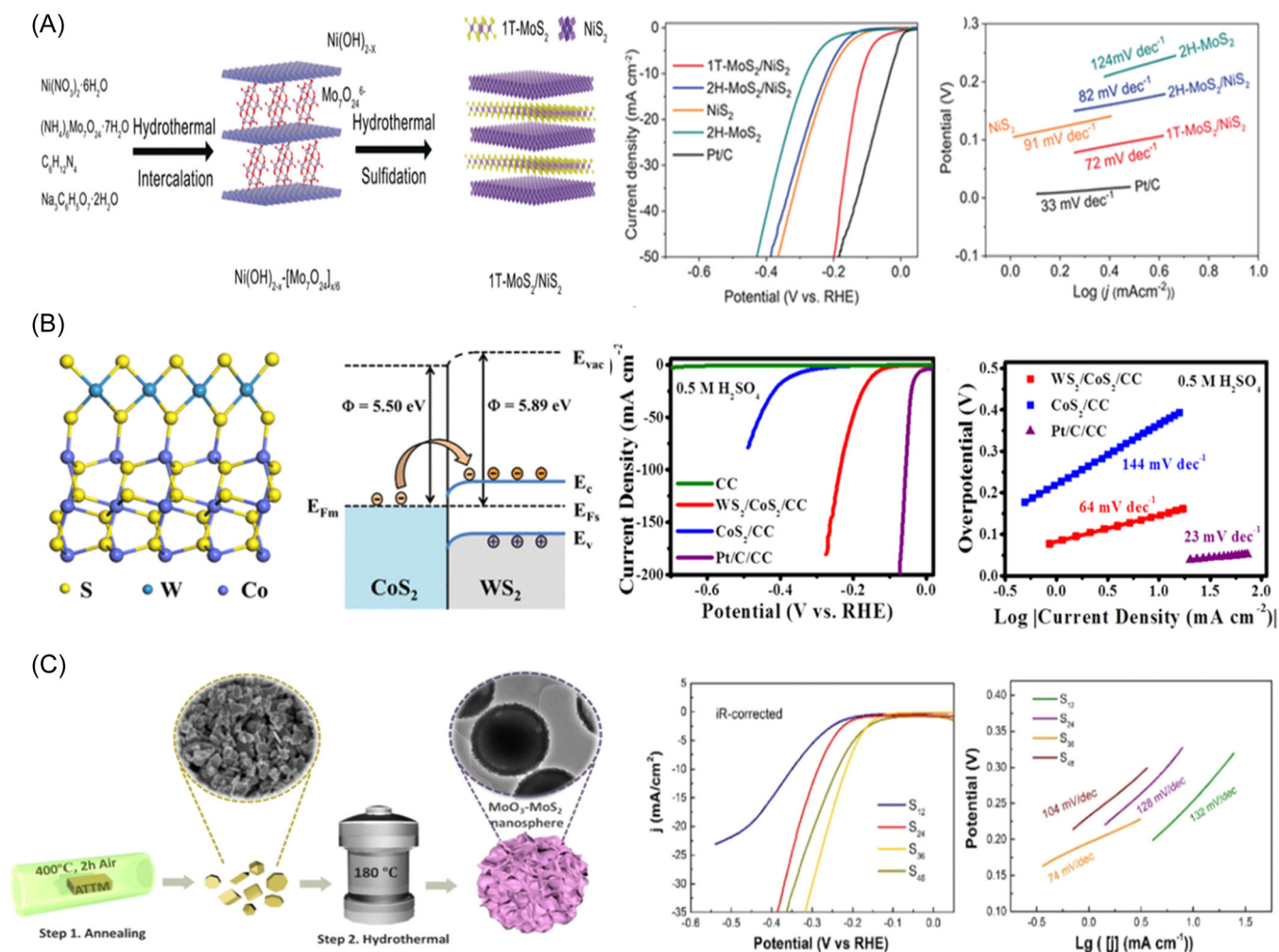


FIGURE 26 (A) 1T-MoS₂/NiS₂ for the HER. Reproduced with permission from Chen et al.,¹⁶² Copyright: 2019 John Wiley and Sons. (B) WS₂/CoS₂ heterostructure catalyst for HER. Reproduced with permission from Wu et al.,¹⁶³ Copyright: 2020 American Chemical Society. And (C) hybrid nanospheres of MoO₃-MoS₂ for HER. Reproduced with permission from Hou et al.¹⁶⁴ Copyright: 2020 Elsevier. HER, hydrogen evolution reaction; PVC, polyvinyl chloride; RHE, reference hydrogen electrode.

technologies have been applied to improve the electrocatalytic activities of MoS₂ and WS₂. With the significant development of high technologies, as well as the critical energy demand for modern life, the prospect of hydrogen energy prepared by catalysts based on MoS₂ and WS₂ could soon become a reality. For those reasons, we believe that catalyst materials based on MoS₂ and WS₂ could be great candidates for energy storage and catalytic applications, especially for HER, in the near future.

ACKNOWLEDGMENTS

This research was supported in part by the National Research Foundation of Korea (NRF) (grant numbers 2017M3D1A1039379, 2021R1A4A3027878, and 2022M3H4A1A01012712). This research was also supported by the Brain Pool Program through the National Research Foundation of Korea (NRF) and funded

by the Ministry of Science and ICT (grant number 2020H1D3A1A04081409).

CONFLICT OF INTEREST STATEMENT

The authors declare no conflict of interest.

ORCID

Soo Young Kim <http://orcid.org/0000-0002-0685-7991>

REFERENCES

- Wang P, Jia C, Huang Y, Duan X. Van der Waals heterostructures by design: from 1D and 2D to 3D. *Matter*. 2021;4(2):552-581.
- Li X, Wang J. One-dimensional and two-dimensional synergized nanostructures for high-performing energy storage and conversion. *InfoMat*. 2020;2(1):3-32.
- Scher JA, Elward JM, Chakraborty A. Shape matters: effect of 1D, 2D, and 3D isovolumetric quantum confinement in

- semiconductor nanoparticles. *J Phys Chem C*. 2016;120(43):24999-25009.
4. Novoselov KS, Mishchenko A, Carvalho A, Castro Neto AH. 2D materials and van der Waals heterostructures. *Science*. 2016;353(6298):aac9439.
 5. Zeng M, Xiao Y, Liu J, Yang K, Fu L. Exploring two-dimensional materials toward the next-generation circuits: from monomer design to assembly control. *Chem Rev*. 2018;118(13):6236-6296.
 6. Glavin NR, Rao R, Varshney V, et al. Emerging applications of elemental 2D materials. *Adv Mater*. 2020;32(7):1904302.
 7. Han SA, Bhatia R, Kim SW. Synthesis, properties and potential applications of two-dimensional transition metal dichalcogenides. *Nano Convergence*. 2015;2(1):17.
 8. Amiin IS, Pu Z, Liu X, et al. Multifunctional Mo-N/C@MoS₂ electrocatalysts for HER, OER, ORR, and Zn-air batteries. *Adv Funct Mater*. 2017;27(44):1702300.
 9. Geim AK, Novoselov KS. The rise of graphene. *Nat Mater*. 2007;6:183-191.
 10. Randviir EP, Brownson DAC, Banks CE. A decade of graphene research: production, applications and outlook. *Mater Today*. 2014;17(9):426-432.
 11. Shearer CJ, Slattery AD, Stapleton AJ, Shapter JG, Gibson CT. Accurate thickness measurement of graphene. *Nanotechnology*. 2016;27(12):125704.
 12. Butler SZ, Hollen SM, Cao L, et al. Progress, challenges, and opportunities in two-dimensional materials beyond graphene. *ACS Nano*. 2013;7(4):2898-2926.
 13. Jing Y, Mu X, Xie C, et al. Enhanced hydrogen evolution reaction of WS₂-CoS₂ heterostructure by synergistic effect. *Int J Hydrogen Energy*. 2019;44(2):809-818.
 14. Prabhu P, Jose V, Lee JM. Design strategies for development of TMD-based heterostructures in electrochemical energy systems. *Matter*. 2020;2(3):526-553.
 15. Frisenda R, Niu Y, Gant P, Muñoz M, Castellanos-Gomez A. Naturally occurring van der Waals materials. *NPJ 2D Mater Appl*. 2020;4(1):38.
 16. Wang H, Li Z, Li D, et al. Van der Waals integration based on two-dimensional materials for high-performance infrared photodetectors. *Adv Funct Mater*. 2021;31(30):2103106.
 17. Yang WX, Zhou H, Su D, et al. Recent progress in 2D material van der Waals heterostructure based luminescence device towards infrared wavelength range. *J Mater Chem C*. 2022;10(19):7352-7367.
 18. Oh SM, Hwang SJ. Recent advances in two-dimensional inorganic nanosheet-based supercapacitor electrodes. *J Korean Ceram Soc*. 2020;57(2):119-134.
 19. Brar VW, Koltonow AR, Huang J. New discoveries and opportunities from two-dimensional materials. *ACS Photonics*. 2017;4(3):407-411.
 20. Rehman SU, Ding ZJ. Enhanced electronic and optical properties of three TMD heterobilayers. *Phys Chem Chem Phys*. 2018;20(24):16604-16614.
 21. Tang X, Kou L. 2D Janus transition metal dichalcogenides: properties and applications. *Phys Status Sol (B)*. 2022;259(4):2100562.
 22. Imani Yengejeh S, Wen W, Wang Y. Mechanical properties of lateral transition metal dichalcogenide heterostructures. *Front Phys*. 2021;16(1):13502.
 23. Chen H, Liu T, Su Z, Shang L, Wei G. 2D transition metal dichalcogenide nanosheets for photo/thermo-based tumor imaging and therapy. *Nanoscale Horiz*. 2018;3(2):74-89.
 24. Hasani A, Tekalgne M, Le QV, Jang HW, Kim SY. Two-dimensional materials as catalysts for solar fuels: hydrogen evolution reaction and CO₂ reduction. *J Mater Chem A*. 2019;7(2):430-454.
 25. Cherusseri J, Choudhary N, Sambath Kumar K, Jung Y, Thomas J. Recent trends in transition metal dichalcogenide based supercapacitor electrodes. *Nanoscale Horiz*. 2019;4(4):840-858.
 26. Chen B, Chao D, Liu E, Jaroniec M, Zhao N, Qiao SZ. Transition metal dichalcogenides for alkali metal ion batteries: engineering strategies at the atomic level. *Energy Environ Sci*. 2020;13(4):1096-1131.
 27. Ping J, Fan Z, Sindoro M, Ying Y, Zhang H. Recent advances in sensing applications of two-dimensional transition metal dichalcogenide nanosheets and their composites. *Adv Funct Mater*. 2017;27(19):1605817.
 28. Xue X, Zhang J, Saana IA, Sun J, Xu Q, Mu S. Rational inert-basal-plane activating design of ultrathin 1T' phase MoS₂ with a MoO₃ heterostructure for enhancing hydrogen evolution performances. *Nanoscale*. 2018;10(35):16531-16538.
 29. Manzeli S, Ovchinnikov D, Pasquier D, Yazyev OV, Kis A. 2D transition metal dichalcogenides. *Nat Rev Mater*. 2017;2(8):17033.
 30. Lv R, Robinson JA, Schaak RE, et al. Transition metal dichalcogenides and beyond: synthesis, properties, and applications of single- and few-layer nanosheets. *Acc Chem Res*. 2015;48(1):56-64.
 31. Yin X, Tang CS, Zheng Y, et al. Recent developments in 2D transition metal dichalcogenides: phase transition and applications of the (quasi-) metallic phases. *Chem Soc Rev*. 2021;50:10087-10115.
 32. Chaves A, Azadani JG, Alsalman H, et al. Bandgap engineering of two-dimensional semiconductor materials. *NPJ 2D Mater Appl*. 2020;4(1):29.
 33. Gusakova J, Wang X, Shiao LL, et al. Electronic properties of bulk and monolayer TMDs: theoretical study within DFT framework (GVJ-2e method). *Phys Status Sol (A)*. 2017;214(12):1700218.
 34. Zhou S, Ning J, Sun J, Srolovitz DJ. Composition-induced type i and direct bandgap transition metal dichalcogenides alloy vertical heterojunctions. *Nanoscale*. 2020;12(1):201-209.
 35. Lee HJ, Lee BJ, Kang D, Jang YJ, Lee JS, Shin HS. 2D materials-based photoelectrochemical cells: combination of transition metal dichalcogenides and reduced graphene oxide for efficient charge transfer. *FlatChem*. 2017;4:54-60.
 36. Zhang Z, Yang M, Zhao N, Wang L, Li Y. Two-dimensional transition metal dichalcogenides as promising anodes for potassium ion batteries from first-principles prediction. *Phys Chem Chem Phys*. 2019;21(42):23441-23446.
 37. Zhu K, Li C, Jing Z, et al. Two-dimensional transition-metal dichalcogenides for electrochemical hydrogen evolution reaction. *FlatChem*. 2019;18:100140.
 38. Liu C, Kong C, Zhang FJ, et al. Research progress of defective MoS₂ for photocatalytic hydrogen evolution. *J Korean Ceram Soc*. 2021;58(2):135-147.

39. Xu H, Zhu J, Ma Q, et al. Two-dimensional MoS₂: structural properties, synthesis methods, and regulation strategies toward oxygen reduction. *Micromachines*. 2021;12(3):240.
40. Mu X, Zhu Y, Gu X, et al. Awakening the oxygen evolution activity of MoS₂ by oxophilic-metal induced surface reorganization engineering. *J Energy Chem*. 2021;62:546-551.
41. Song J, Wei C, Huang Z-F, et al. A review on fundamentals for designing oxygen evolution electrocatalysts. *Chem Soc Rev*. 2020;49(7):2196-2214.
42. Maghirang AB, Huang ZQ, Villaos RAB, et al. Predicting two-dimensional topological phases in Janus materials by substitutional doping in transition metal dichalcogenide monolayers. *NPJ 2D Mater Appl*. 2019;3(1):35.
43. Ghatak K, Kang KN, Yang E-H, Datta D. Controlled edge dependent stacking of WS₂-WS₂ homo- and WS₂-WSe₂ hetero-structures: a computational study. *Sci Rep*. 2020;10(1):1648.
44. Geim AK, Grigorieva IV. Van der Waals heterostructures. *Nature*. 2013;499(7459):419-425.
45. Suryawanshi SR, Kolhe PS, Rout CS, Late DJ, More MA. Spectral analysis of the emission current noise exhibited by few layer WS₂ nanosheets emitter. *Ultramicroscopy*. 2015;149:51-57.
46. Radisavljevic B, Radenovic A, Brivio J, Giacometti V, Kis A. Single-layer MoS₂ transistors. *Nat Nanotechnol*. 2011;6(3):147-150.
47. Yue M, Lambert H, Pahon E, Roche R, Jemei S, Hissel D. Hydrogen energy systems: a critical review of technologies, applications, trends and challenges. *Renewable Sustainable Energy Rev*. 2021;146:111180.
48. Staffell I, Scamman D, Abad AV, et al. The role of hydrogen and fuel cells in the global energy system. *Energy Environ Sci*. 2019;12(2):463-491.
49. Qi J, Zhang W, Cao R. Solar-to-hydrogen energy conversion based on water splitting. *Adv Energy Mater*. 2018;8(5):1701620.
50. Kumar A, Kim I-H, Mathur L, Kim H-S, Song SJ. Design of tin polyphosphate for hydrogen evolution reaction and supercapacitor applications. *J Korean Ceram Soc*. 2021;58(6):688-699.
51. Liu S, Zhou L, Zhang W, et al. Stabilizing sulfur vacancy defects by performing "click" chemistry of ultrafine palladium to trigger a high-efficiency hydrogen evolution of MoS₂. *Nanoscale*. 2020;12(18):9943-9949.
52. Anantharaj S, Ede SR, Sakthikumar K, Karthick K, Mishra S, Kundu S. Recent trends and perspectives in electrochemical water splitting with an emphasis on sulfide, selenide, and phosphide catalysts of Fe, Co, and Ni: a review. *ACS Catal*. 2016;6(12):8069-8097.
53. Vikraman D, Hussain S, Akbar K, et al. Improved hydrogen evolution reaction performance using MoS₂-WS₂ heterostructures by physicochemical process. *ACS Sustainable Chem Eng*. 2018;6(7):8400-8409.
54. Toh RJ, Sofer Z, Luxa J, Sedmidubský D, Pumera M. 3R phase of MoS₂ and WS₂ outperforms the corresponding 2H phase for hydrogen evolution. *Chem Commun*. 2017;53(21):3054-3057.
55. Wang T, Wang P, Pang Y, et al. Vertically mounting molybdenum disulfide nanosheets on dimolybdenum carbide nanomeshes enables efficient hydrogen evolution. *Nano Res*. 2022;15(5):3946-3951.
56. Li W, Liu G, Li J, et al. Hydrogen evolution reaction mechanism on 2H-MoS₂ electrocatalyst. *Appl Surf Sci*. 2019;498:143869.
57. Xia L, Pan K, Wu H, et al. Few-layered WS₂ anchored on Co, N-doped carbon hollow polyhedron for oxygen evolution and hydrogen evolution. *ACS Appl Mater Interfaces*. 2022;14(19):22030-22040.
58. Voiry D, Salehi M, Silva R, et al. Conducting MoS₂ nanosheets as catalysts for hydrogen evolution reaction. *Nano Lett*. 2013;13(12):6222-6227.
59. Pan Y, Zheng F, Wang X, et al. Enhanced electrochemical hydrogen evolution performance of WS₂ nanosheets by Te doping. *J Catal*. 2020;382:204-211.
60. Strmcnik D, Uchimura M, Wang C, et al. Improving the hydrogen oxidation reaction rate by promotion of hydroxyl adsorption. *Nat Chem*. 2013;5(4):300-306.
61. Ifkovits ZP, Evans JM, Meier MC, Papadantonakis KM, Lewis NS. Decoupled electrochemical water-splitting systems: a review and perspective. *Energy Environ Sci*. 2021;14(9):4740-4759.
62. Li P, Li J, Feng X, et al. Metal-organic frameworks with photocatalytic bactericidal activity for integrated air cleaning. *Nat Commun*. 2019;10(1):2177.
63. Zhang J, Zhang Q, Feng X. Support and interface effects in water-splitting electrocatalysts. *Adv Mater*. 2019;31(31):1808167.
64. Xiong J, Yan C, Liu W, et al. Insights into the principles, design methodology and applications of electrocatalysts towards hydrogen evolution reaction. *Energy Rep*. 2021;7:8577-8596.
65. Li X, Zhao L, Yu J, et al. Water splitting: from electrode to green energy system. *Nano Micro Lett*. 2020;12(1):131.
66. Shinagawa T, Takanabe K. Towards versatile and sustainable hydrogen production through electrocatalytic water splitting: electrolyte engineering. *ChemSusChem*. 2017;10(7):1318-1336.
67. Peng J, Dong W, Wang Z, et al. Recent advances in 2D transition metal compounds for electrocatalytic full water splitting in neutral media. *Mater Today Adv*. 2020;8:100081.
68. Hona RK, Karki SB, Cao T, Mishra R, Sterbinsky GE, Ramezanipour F. Sustainable oxide electrocatalyst for hydrogen- and oxygen-evolution reactions. *ACS Catal*. 2021;11(23):14605-14614.
69. Akbashev AR. Electrocatalysis goes nuts. *ACS Catal*. 2022;12(8):4296-4301.
70. Ouimet RJ, Glenn JR, De Porcellinis D, Motz AR, Carmo M, Ayers KE. The role of electrocatalysts in the development of gigawatt-scale PEM electrolyzers. *ACS Catal*. 2022;12:6159-6171.
71. Wang S, Lu A, Zhong CJ. Hydrogen production from water electrolysis: role of catalysts. *Nano Convergence*. 2021;8(1):4.
72. Lasia A. Mechanism and kinetics of the hydrogen evolution reaction. *Int J Hydrogen Energy*. 2019;44(36):19484-19518.
73. Bao F, Kemppainen E, Dorbandt I, et al. Understanding the hydrogen evolution reaction kinetics of electrodeposited nickel-molybdenum in acidic, near-neutral, and alkaline conditions. *ChemElectroChem*. 2021;8(1):195-208.

74. Long G, Wan K, Liu M, Liang Z, Piao J, Tsiakaras P. Active sites and mechanism on nitrogen-doped carbon catalyst for hydrogen evolution reaction. *J Catal.* 2017;348:151-159.
75. Sarma PV, Kayal A, Sharma CH, Thalakulam M, Mitra J, Shaijumon MM. Electrocatalysis on edge-rich spiral WS₂ for hydrogen evolution. *ACS Nano.* 2019;13(9):10448-10455.
76. Zhou H, Yu F, Sun J, et al. Highly active and durable self-standing WS₂/graphene hybrid catalysts for the hydrogen evolution reaction. *J Mater Chem A.* 2016;4(24):9472-9476.
77. Mansingh S, Das KK, Parida K. HERs in an acidic medium over MoS₂ nanosheets: from fundamentals to synthesis and the recent progress. *Sustainable Energy Fuels.* 2021;5(7):1952-1987.
78. Li G, Zhang D, Qiao Q, et al. All the catalytic active sites of MoS₂ for hydrogen evolution. *J Am Chem Soc.* 2016;138(51):16632-16638.
79. Tang Q, Jiang D. Mechanism of hydrogen evolution reaction on 1T-MoS₂ from first principles. *ACS Catal.* 2016;6(8):4953-4961.
80. Chen Z, Duan X, Wei W, Wang S, Ni BJ. Recent advances in transition metal-based electrocatalysts for alkaline hydrogen evolution. *J Mater Chem A.* 2019;7(25):14971-15005.
81. Wei J, Zhou M, Long A, et al. Heterostructured electrocatalysts for hydrogen evolution reaction under alkaline conditions. *Nano Micro Lett.* 2018;10(4):75.
82. Zeng M, Li Y. Recent advances in heterogeneous electrocatalysts for the hydrogen evolution reaction. *J Mater Chem A.* 2015;3(29):14942-14962.
83. Gao Q, Zhang W, Shi Z, Yang L, Tang Y. Structural design and electronic modulation of transition-metal-carbide electrocatalysts toward efficient hydrogen evolution. *Adv Mater.* 2019;31(2):1802880.
84. Yu P, Wang F, Shifa TA, et al. Earth abundant materials beyond transition metal dichalcogenides: a focus on electrocatalyzing hydrogen evolution reaction. *Nano Energy.* 2019;58:244-276.
85. Prats H, Chan K. The determination of the HOR/HER reaction mechanism from experimental kinetic data. *Phys Chem Chem Phys.* 2021;23(48):27150-27158.
86. Rheinländer PJ, Herranz J, Durst J, Gasteiger HA. Kinetics of the hydrogen oxidation/evolution reaction on polycrystalline platinum in alkaline electrolyte reaction order with respect to hydrogen pressure. *J Electrochem Soc.* 2014;161(14):F1448-F1457.
87. Shinagawa T, Garcia-Esparza AT, Takanabe K. Insight on Tafel slopes from a microkinetic analysis of aqueous electrocatalysis for energy conversion. *Sci Rep.* 2015;5(1):13801.
88. Chung CC, Narra S, Jokar E, Wu HP, Wei-Guang diau E. Inverted planar solar cells based on perovskite/graphene oxide hybrid composites. *J Mater Chem A.* 2017;5(27):13957-13965.
89. Fei H, Dong J, Arellano-Jiménez MJ, et al. Atomic cobalt on nitrogen-doped graphene for hydrogen generation. *Nat Commun.* 2015;6(1):8668.
90. Kozuch S, Martin JM. "Turning Over" Definitions in Catalytic Cycles. Vol 2. ACS Publications; 2012:2787-2794.
91. Anantharaj S, Karthik PE, Noda S. The significance of properly reporting turnover frequency in electrocatalysis research. *Angew Chem Int Ed.* 2021;60(43):23051-23067.
92. Shin S, Jin Z, Kwon DH, Bose R, Min YS. High turnover frequency of hydrogen evolution reaction on amorphous MoS₂ thin film directly grown by atomic layer deposition. *Langmuir.* 2015;31(3):1196-1202.
93. Xie H, Xiong X. A porous molybdenum disulfide and reduced graphene oxide nanocomposite (MoS₂-rGO) with high adsorption capacity for fast and preferential adsorption towards Congo red. *J Environ Chem Eng.* 2017;5(1):1150-1158.
94. Nguyen TV, Le QV, Nguyen CC, et al. Synthesis of nanocoral tungsten carbide/carbon fibers as efficient catalysts for hydrogen evolution reaction. *Int J Energy Res.* 2022;46(9):13089-13098.
95. Gong Q, Wang Y, Hu Q, et al. Ultrasmall and phase-pure W₂C nanoparticles for efficient electrocatalytic and photoelectrochemical hydrogen evolution. *Nat Commun.* 2016;7(1):13216.
96. Van Nguyen T, Tekalgne M, Nguyen TP, et al. Control of the morphologies of molybdenum disulfide for hydrogen evolution reaction. *Int J Energy Res.* 2022;46(8):11479-11491.
97. Van Nguyen T, Do HH, Tekalgne M, et al. WS₂-WC-WO₃ nano-hollow spheres as an efficient and durable catalyst for hydrogen evolution reaction. *Nano Convergence.* 2021;8(1):1-12.
98. Choudhary N, Park J, Hwang JY, et al. Centimeter scale patterned growth of vertically stacked few layer only 2D MoS₂/WS₂ van der Waals heterostructure. *Sci Rep.* 2016;6(1):25456.
99. Tsuppayakorn-ae P, Pungtrakool W, Pinsook U, Bovornratanaraks T. The minimal supercells approach for ab-initio calculation in 2D alloying transition metal dichalcogenides with special quasi-random structure. *Mater Res Express.* 2020;7(8):086502.
100. Li M, Shi J, Liu L, Yu P, Xi N, Wang Y. Experimental study and modeling of atomic-scale friction in zigzag and armchair lattice orientations of MoS₂. *Sci Technol Adv Mater.* 2016;17(1):189-199.
101. Yelgel C, Yelgel ÖC, Gülseren O. Structural and electronic properties of MoS₂, WS₂, and WS₂/MoS₂ heterostructures encapsulated with hexagonal boron nitride monolayers. *J Appl Phys.* 2017;122(6):065303.
102. Cotrufo M, Sun L, Choi J, Alù A, Li X. Enhancing functionalities of atomically thin semiconductors with plasmonic nanostructures. *Nanophotonics.* 2019;8(4):577-598.
103. Coogan Á, Gun'ko YK. Solution-based "bottom-up" synthesis of group VI transition metal dichalcogenides and their applications. *Mater Adv.* 2021;2(1):146-164.
104. Kuc A, Zibouche N, Heine T. Influence of quantum confinement on the electronic structure of the transition metal sulfide TS₂. *Phys Rev B: Condens Matter Mater Phys.* 2011;83(24):245213.
105. Ho TA, Bae C, Lee S, et al. Edge-on MoS₂ thin films by atomic layer deposition for understanding the interplay between the active area and hydrogen evolution reaction. *Chem Mater.* 2017;29(17):7604-7614.
106. Balasubramanyam S, Shirazi M, Bloodgood MA, et al. Edge-site nanoengineering of WS₂ by low-temperature plasma-enhanced atomic layer deposition for electrocatalytic hydrogen evolution. *Chem Mater.* 2019;31(14):5104-5115.

107. Yeo S, Nandi DK, Rahul R, et al. Low-temperature direct synthesis of high quality WS₂ thin films by plasma-enhanced atomic layer deposition for energy related applications. *Appl Surf Sci.* 2018;459:596-605.
108. Yang H, Wang Y, Zou X, et al. Growth mechanisms and morphology engineering of atomic layer-deposited WS₂. *ACS Appl Mater Interfaces.* 2021;13(36):43115-43122.
109. Tan LK, Liu B, Teng JH, Guo S, Low HY, Loh KP. Atomic layer deposition of a MoS₂ film. *Nanoscale.* 2014;6(18):10584-10588.
110. Li H, Wu J, Yin Z, Zhang H. Preparation and applications of mechanically exfoliated single-layer and multilayer MoS₂ and WSe₂ nanosheets. *Acc Chem Res.* 2014;47(4):1067-1075.
111. Liu J, Lo TW, Sun J, Yip CT, Lam CH, Lei DY. A comprehensive comparison study on the vibrational and optical properties of CVD-grown and mechanically exfoliated few-layered. *J Mater Chem C.* 2017;5(43):11239-11245.
112. Desai JA, Adhikari N, Kaul AB. Chemical exfoliation efficacy of semiconducting WS₂ and its use in an additively manufactured heterostructure graphene-WS₂-graphene photodiode. *RSC Adv.* 2019;9(44):25805-25816.
113. Eda G, Yamaguchi H, Voiry D, Fujita T, Chen M, Chhowalla M. Photoluminescence from chemically exfoliated MoS₂. *Nano Lett.* 2011;11(12):5111-5116.
114. Er E, Hou HL, Criado A, et al. High-yield preparation of exfoliated 1T-MoS₂ with SERS activity. *Chem Mater.* 2019;31(15):5725-5734.
115. Leong SX, Mayorga-Martinez CC, Chia X, Luxa J, Sofer Z, Pumera M. 2H→1T phase change in direct synthesis of WS₂ nanosheets via solution-based electrochemical exfoliation and their catalytic properties. *ACS Appl Mater Interfaces.* 2017;9(31):26350-26356.
116. Abd-Elrahim AG, Chun DM. One-step mechanical exfoliation and deposition of layered materials (graphite, MoS₂, and BN) by vacuum-kinetic spray process. *Vacuum.* 2022;196:110732.
117. Huang J, Liu Y, Yan P, Gao J, Fan Y, Jiang W. Mechanically exfoliated MoS₂ nanoflakes for optimizing the thermoelectric performance of SrTiO₃-based ceramic composites. *J Materiomics.* 2022;8(4):790-798.
118. Kim TI, Kim J, Park IJ, Cho KO, Choi SY. Chemically exfoliated 1T-phase transition metal dichalcogenide nanosheets for transparent antibacterial applications. *2D Mater.* 2019;6(2):025025.
119. Zhang Y, Chen X, Zhang H, et al. Facile exfoliation for high-quality molybdenum disulfide nanoflakes and relevant field-effect transistors developed with thermal treatment. *Front Chem.* 2021;9:650901.
120. Lin H, Wang J, Luo Q, et al. Rapid and highly efficient chemical exfoliation of layered MoS₂ and WS₂. *J Alloys Compd.* 2017;699:222-229.
121. Muralikrishna S, Manjunath K, Samrat D, Reddy V, Ramakrishnappa T, Nagaraju DH. Hydrothermal synthesis of 2D MoS₂ nanosheets for electrocatalytic hydrogen evolution reaction. *RSC Adv.* 2015;5(109):89389-89396.
122. Vattikuti SVP, Byon C, Chitturi V. Selective hydrothermally synthesis of hexagonal WS₂ platelets and their photocatalytic performance under visible light irradiation. *Superlattices Microstruct.* 2016;94:39-50.
123. He Z, Guo Z, Wa Q, Zhong X, Wang X, Chen Y. NiSx@MoS₂ heterostructure prepared by atomic layer deposition as high-performance hydrogen evolution reaction electrocatalysts in alkaline media. *J Mater Res.* 2020;35(7):822-830.
124. Yang J, Zhu J, Xu J, Zhang C, Liu T. MoSe₂ nanosheet array with layered MoS₂ heterostructures for superior hydrogen evolution and lithium storage performance. *ACS Appl Mater Interfaces.* 2017;9(51):44550-44559.
125. Zou Y, Shi JW, Ma D, et al. WS₂/graphitic carbon nitride heterojunction nanosheets decorated with CdS quantum dots for photocatalytic hydrogen production. *ChemSusChem.* 2018;11(7):1187-1197.
126. Jiang X, Sun B, Song Y, Dou M, Ji J, Wang F. One-pot synthesis of MoS₂/WS₂ ultrathin nanoflakes with vertically aligned structure on indium tin oxide as a photocathode for enhanced photo-assistant electrochemical hydrogen evolution reaction. *RSC Adv.* 2017;7(78):49309-49319.
127. Swathi S, Yuvakkumar R, Senthilkumar P, Ravi G, Velauthapillai D. Surfactant-assisted tungsten sulfide mesoporous sphere for hydrogen production. *Int J Hydrogen Energy.* 2022;47(100):41984-41993.
128. Yang J, Voiry D, Ahn SJ, et al. Two-dimensional hybrid nanosheets of tungsten disulfide and reduced graphene oxide as catalysts for enhanced hydrogen evolution. *Angew Chem Int Ed.* 2013;125(51):13996-13999.
129. Ren X, Pang L, Zhang Y, Ren X, Fan H, Liu S. One-step hydrothermal synthesis of monolayer MoS₂ quantum dots for highly efficient electrocatalytic hydrogen evolution. *J Mater Chem A.* 2015;3(20):10693-10697.
130. Nadeem Riaz K, Yousaf N, Bilal Tahir M, Israr Z, Iqbal T. Facile hydrothermal synthesis of 3D flower-like La-MoS₂ nanostructure for photocatalytic hydrogen energy production. *Int J Energy Res.* 2019;43(1):491-499.
131. Jeon J, Jang SK, Jeon SM, et al. Layer-controlled CVD growth of large-area two-dimensional MoS₂ films. *Nanoscale.* 2015;7(5):1688-1695.
132. Shi B, Zhou D, Qiu R, et al. High-efficiency synthesis of large-area monolayer WS₂ crystals on SiO₂/Si substrate via NaCl-assisted atmospheric pressure chemical vapor deposition. *Appl Surf Sci.* 2020;533:147479.
133. Soram BS, Dai JY, Thangjam IS, Kim NH, Lee JH. One-step electrodeposited MoS₂@Ni-mesh electrode for flexible and transparent asymmetric solid-state supercapacitors. *J Mater Chem A.* 2020;8(45):24040-24052.
134. Pu Z, Liu Q, Asiri AM, Obaid AY, Sun X. One-step electrodeposition fabrication of graphene film-confined WS₂ nanoparticles with enhanced electrochemical catalytic activity for hydrogen evolution. *Electrochim Acta.* 2014;134:8-12.
135. Modtland BJ, Navarro-Moratalla E, Ji X, Baldo M, Kong J. Monolayer tungsten disulfide (WS₂) via chlorine-driven chemical vapor transport. *Small.* 2017;13(33):1701232.
136. Rigi VJC, Jayaraj MK, Saji KJ. Envisaging radio frequency magnetron sputtering as an efficient method for large scale deposition of homogeneous two dimensional MoS₂. *Appl Surf Sci.* 2020;529:147158.
137. Nakayasu Y, Kobayashi H, Katahira S, Tomai T, Honma I. Rapid, one-step fabrication of MoS₂ electrocatalysts by hydrothermal electrodeposition. *Electrochem Commun.* 2022;134:107180.

138. Nguyen TP, Nguyen DLT, Nguyen VH, et al. Facile synthesis of WS₂ hollow spheres and their hydrogen evolution reaction performance. *Appl Surf Sci.* 2020;505:144574.
139. Van Nguyen T, Nguyen TP, Van Le Q, Van Dao D, Ahn SH, Kim SY. Synthesis of very small molybdenum disulfide nanoflowers for hydrogen evolution reaction. *Appl Surf Sci.* 2022;607:154979.
140. Wang X, Zhang Y, Si H, et al. Single-atom vacancy defect to trigger high-efficiency hydrogen evolution of MoS₂. *J Am Chem Soc.* 2020;142(9):4298-4308.
141. Jiang L, Zhou Q, Li JJ, Xia YX, Li HX, Li YJ. Engineering isolated S vacancies over 2D MoS₂ basal planes for catalytic hydrogen evolution. *ACS Appl Nano Mater.* 2022;5(3):3521-3530.
142. Kong C, Han YX, Hou L, Yan PJ. The distribution effect of sulfur vacancy in 2H-MoS₂ monolayer on its H₂ generation mechanism from density functional theory. *Int J Hydrogen Energy.* 2022;47(1):242-249.
143. Ye G, Gong Y, Lin J, et al. Defects engineered monolayer MoS₂ for improved hydrogen evolution reaction. *Nano Lett.* 2016;16(2):1097-1103.
144. Wu L, Van Hoof AJF, Dzade NY, et al. Enhancing the electrocatalytic activity of 2H-WS₂ for hydrogen evolution via defect engineering. *Phys Chem Chem Phys.* 2019;21(11):6071-6079.
145. Hasani A, Nguyen TP, Tekalgne M, et al. The role of metal dopants in WS₂ nanoflowers in enhancing the hydrogen evolution reaction. *Appl Catal A.* 2018;567:73-79.
146. Shi Y, Zhou Y, Yang DR, et al. Energy level engineering of MoS₂ by transition-metal doping for accelerating hydrogen evolution reaction. *J Am Chem Soc.* 2017;139(43):15479-15485.
147. Xie J, Zhang J, Li S, et al. Controllable disorder engineering in oxygen-incorporated MoS₂ ultrathin nanosheets for efficient hydrogen evolution. *J Am Chem Soc.* 2013;135(47):17881-17888.
148. Ren X, Yang F, Chen R, Ren P, Wang Y. Improvement of HER activity for MoS₂: insight into the effect and mechanism of phosphorus post-doping. *New J Chem.* 2020;44(4):1493-1499.
149. Li R, Yang L, Xiong T, et al. Nitrogen doped MoS₂ nanosheets synthesized via a low-temperature process as electrocatalysts with enhanced activity for hydrogen evolution reaction. *J Power Sources.* 2017;356:133-139.
150. Sun C, Zhang J, Ma J, et al. N-doped WS₂ nanosheets: a high-performance electrocatalyst for the hydrogen evolution reaction. *J Mater Chem A.* 2016;4(29):11234-11238.
151. Sun L, Gao M, Jing Z, et al. 1 T-Phase enriched P doped WS₂ nanosphere for highly efficient electrochemical hydrogen evolution reaction. *Chem Eng J.* 2022;429:132187.
152. Fan X, Xu P, Zhou D, et al. Fast and efficient preparation of exfoliated 2H MoS₂ nanosheets by sonication-assisted lithium intercalation and infrared laser-induced 1T to 2H phase reversion. *Nano Lett.* 2015;15(9):5956-5960.
153. Ambrosi A, Sofer Z, Pumera M. 2H → 1T phase transition and hydrogen evolution activity of MoS₂, MoSe₂, WS₂ and WSe₂ strongly depends on the MX₂ composition. *Chem Commun.* 2015;51(40):8450-8453.
154. Jiang Y, Li S, Zhang F, Zheng W, Zhao L, Feng Q. Metal-semiconductor 1T/2H-MoS₂ by a heteroatom-doping strategy for enhanced electrocatalytic hydrogen evolution. *Catal Commun.* 2021;156:106325.
155. Li W, Shen Y, Xiao X, et al. Simple Te-thermal converting 2H to 1T@2H MoS₂ homojunctions with enhanced supercapacitor performance. *ACS Appl Energy Mater.* 2019;2(11):8337-8344.
156. Gan X, Lee LYS, Wong K, et al. 2H/1T phase transition of multilayer MoS₂ by electrochemical incorporation of S vacancies. *ACS Appl Energy Mater.* 2018;1(9):4754-4765.
157. Zhang K, Jin B, Gao Y, et al. Aligned heterointerface-induced 1T-MoS₂ monolayer with near-ideal Gibbs free for stable hydrogen evolution reaction. *Small.* 2019;15(8):1804903.
158. Lukowski MA, Daniel AS, English CR, et al. Highly active hydrogen evolution catalysis from metallic WS₂ nanosheets. *Energy Environ Sci.* 2014;7(8):2608-2613.
159. Shifa TA, Wang F, Cheng Z, et al. A vertical-oriented WS₂ nanosheet sensitized by graphene: an advanced electrocatalyst for hydrogen evolution reaction. *Nanoscale.* 2015;7(35):14760-14765.
160. Li Y, Wang H, Xie L, Liang Y, Hong G, Dai H. MoS₂ nanoparticles grown on graphene: an advanced catalyst for the hydrogen evolution reaction. *J Am Chem Soc.* 2011;133(19):7296-7299.
161. Lu T, Li T, Shi D, et al. In situ establishment of Co/MoS₂ heterostructures onto inverse opal-structured N, S-doped carbon hollow nanospheres: interfacial and architectural dual engineering for efficient hydrogen evolution reaction. *SmartMat.* 2021;2(4):591-602.
162. Chen X, Wang Z, Wei Y, et al. High phase-purity 1T-MoS₂ ultrathin nanosheets by a spatially confined template. *Angew Chem Int Ed.* 2019;58(49):17621-17624.
163. Wu J, Chen T, Zhu C, et al. Rational construction of a WS₂/CoS₂ heterostructure electrocatalyst for efficient hydrogen evolution at all pH values. *ACS Sustainable Chem Eng.* 2020;8(11):4474-4480.
164. Hou X, Mensah A, Zhao M, Cai Y, Wei Q. Facile controlled synthesis of monodispersed MoO₃-MoS₂ hybrid nanospheres for efficient hydrogen evolution reaction. *Appl Surf Sci.* 2020;529:147115.

AUTHOR BIOGRAPHIES



Tuan Van Nguyen reaction. received the M.Sc. degree in chemical engineering from School of Chemical Engineering, Ha Noi University of Science and Technology, Viet Nam, in 2018. Since 2019, under the guidance of professor Soo Young Kim and professor Sang Hyun Ahn, he is currently pursuing his Ph.D. degree at Chung-Ang University, South Korea. His major focus on the electrochemical application of transition metal materials, such as electrochromic device and hydrogen evolution



Sang Hyun Ahn received his Ph.D. degree in School of Chemical and Biological Engineering of Seoul National University in 2012. After that he joined Thomas Moffat's group as postdoctoral researcher in National Institute of Standard and Technology, the USA. Currently, he is an associate professor in School of Chemical Engineering and Material Science of Chung-Ang University. His research focuses on electrochemical materials and devices for energy conversion and storage, including water, carbon dioxide, and ammonia electrolysis.



Soo Young Kim received the Ph.D. degree in materials science and engineering from Pohang University of Science and Technology, Pohang, South Korea, in 2007. After his postdoctoral period in Georgia Institute of

Technology, the USA, he joined Chung-Ang University in 2009. Currently, he is a professor in Department of Materials Science and Engineering of Korea University. He is interested in the modulation of the properties of 2D materials, such as graphene, graphene oxide, transition metal dichalcogenides, and halide perovskites, and their applications to various devices, such as organic photovoltaics, perovskite solar cells, light emitting diodes, and gas sensors.

How to cite this article: Van Nguyen T, Tekalgne M, Nguyen TP, Van Le Q, Ahn SH, Kim SY. Electrocatalysts based on MoS₂ and WS₂ for hydrogen evolution reaction: an overview. *Battery Energy*. 2023;2:20220057. [doi:10.1002/bte2.20220057](https://doi.org/10.1002/bte2.20220057)